

BKHP Report

William Wang

Alongside Gordon Peiker, worked on this project from June 22 to August 22 as an summer REU student. The project tackled resolving $\text{Ba}_{3-x}\text{K}_x\text{H}_x(\text{PO}_4)_2$'s conductivity and exploring the ball mill as an alternative synthesis mechanism.

August 22, 2025

Contents

1. Introduction	4
1.1. Conductivity	4
1.2. Ball Mill Synthesis	4
2. Conductivity	5
2.1. Milling Samples	5
2.1.1. Diffraction Results	5
2.1.2. Confocal Microscopy Results	6
2.1.2.1. Pre-Mill	7
2.1.2.2. Post Planetary Milling	7
2.1.2.3. Post Planetary & High Energy Milling	8
2.1.2.4. Confocal Microscopy Comments	8
2.1.3. Dynamic Light Scattering Results	9
2.1.3.1. Sample Preparation	9
2.1.3.2. Dynamic Light Scattering Comments	9
2.2. Making Pellets	9
2.3. EIS Measurements	10
2.3.1. $100 \rightarrow 250^\circ\text{C}$ & Initial Ambient Measurement Pellets	10
2.3.2. $100 \rightarrow 250^\circ\text{C}$ Measurements	10
2.3.2.1. Capacitance Analysis	12
2.3.3. Ambient Measurements	12
2.3.4. TGA & DSC Data	13
2.3.5. Ambient Hydration Behavior & Intermediate Temperature Pellets	13
2.3.6. Ambient Hydration Behavior	14
2.3.7. Intermediate Temperature Measurements	14
2.3.8. Intermediate Temperature Transition	15
2.3.9. Bode Plot Comments	17
2.4. Humid Measurements	17
2.5. Future Work	19
3. Ball Mill Synthesis	20
3.1. Mill Synthesis Preparation	20
3.1.1. Synthesis Mechanism	20
3.1.2. Synthesis Setup	20
3.1.3. $\text{Ba}_3(\text{PO}_4)_2$ Impurity Phase	20
3.1.4. Steel Impurities	22
3.2. Determining Potassium Detection Limit	22
3.2.1. $x = 1$ Synthesis Replication	22
3.2.2. $x = 2$ Synthesis	24
3.3. Characterizing Washed $x = 2$ Sample	25
3.3.1. Potassium Occupancy Refinement	25
3.3.2. Lattice Parameter Analysis	26
3.3.3. Proton Nuclear Magnetic Resonance Spectroscopy	26
3.3.4. Washing for Potassium	27
3.3.5. $x = 1$ Milled Synthesis Pellet	27

3.4. Future Work	28
4. Acknowledgements	29
5. Referenced Data	30
5.1. Single Crystal Confocal Microscope Images	30
5.1.1. Planetary Milled Pellet Intermediate Temperature Measurements	31
5.1.2. First $x = 1$ Synthesis	32
6. Miscellaneous Documents	33
6.1. Ba ₂ KH(PO ₄) ₂ Synthesis Instructions	33
6.1.1. At a glance	33
6.1.2. Step-by-Step Instructions	33
6.1.3. Synthesizing with Stored Potassium Bearing Solution	33
6.2. Confocal Microscopy Sample Preparation Instructions	34
6.2.1. Step-by-Step Instructions	34
Index of Figures	35
Index of Tables	36

1. Introduction

The project aimed to resolve two major questions about BKHP:

1. Investigating the material's bulk conductivity
2. Determining the feasibility of the ball mill as a synthesis method

The material is of particular interest since it is insoluble as a proton conductor and is always in its trigonal space group.

1.1. Conductivity

BKHP's low conductivity ($2.4 \times 10^{-5} \frac{\text{S}}{\text{cm}}$ for $x = 0.80$ at 250°C) compared to other superprotonic materials was an open question in the group since the original paper was published by Chrisholm et. al. in the 2010s.

Recent molecular dynamics simulations by the group's collaborators (Kozinsky Group) have suggested that BKHP conductivity may be anisotropic and minimal along the z-axis.

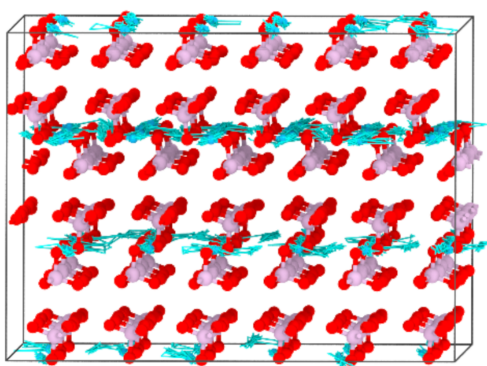


Figure 1: BKHP Proton Hopping

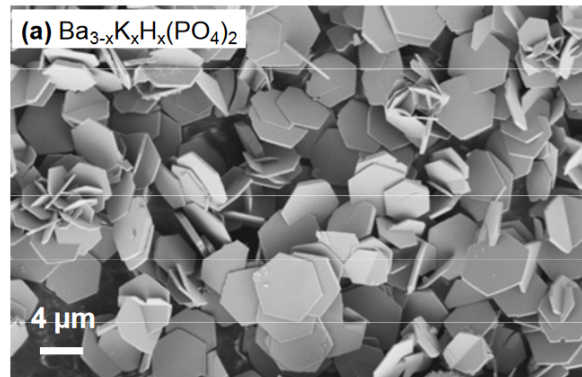


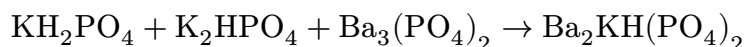
Figure 2: SEM BKHP Image

Due to the platelet structure that is formed in a typical aqueous synthesis, once the material is pressed into a pellet, the z-direction conductivity is overrepresented. The original research plan was to utilize the ball mill to form smaller crystallites with a more randomized orientation, which one pressed into a pellet would recover the "true" bulk conductivity.

1.2. Ball Mill Synthesis

The traditional aqueous BKHP synthesis method involves producing a 14.6M solution of di-potassium phosphate to produce a total of $\approx 0.8\text{g}$ of sample. Producing BKHP in the ball mill would prove a more sustainable, less intensive, and solvent-free method.

The method proposed involves milling two potassium precursors with barium phosphate to produce an $x = 1$ stoichiometry BKHP:



2. Conductivity

2.1. Milling Samples

BKHP was synthesized via the typical aqueous synthesis procedure outlined below. Two separate milled samples were produced. One sample was milled only in the planetary mill. The other sample was first milled in the planetary mill and then in the high energy mill.

- Planetary Mill: 8 large, 7 medium, 23, small zirconia balls for 2 hours
- High Energy Mill: 2 large and 2 small steel balls for 2 hours

Powder diffraction data collected on BKHP sample before and after each phase of milling.

2.1.1. Diffraction Results

Lattice and size parameters from these refinements are likely not the most accurate or can't be confirmed. Recommended to mix sample with silicon or other reference material for accurate determination of lattice parameters. Regardless, the results were not particularly helpful.

Considered peak broadening (\rightarrow particle size reduction) & change in intensity pre/post mill.

SAMPLE	SIZE (μm)	a (Å)	c (Å)
Pre-Mill	0.0616	5.67021	21.04793
Post-Planetary Mill	0.0428	5.67151	21.05562
Post Planetary Mill w/Si	0.0458	5.68219	21.11067
Post High-Energy Mill	0.026	5.65661	21.05575

Table 1: Diffraction Lattice & Size Parameters

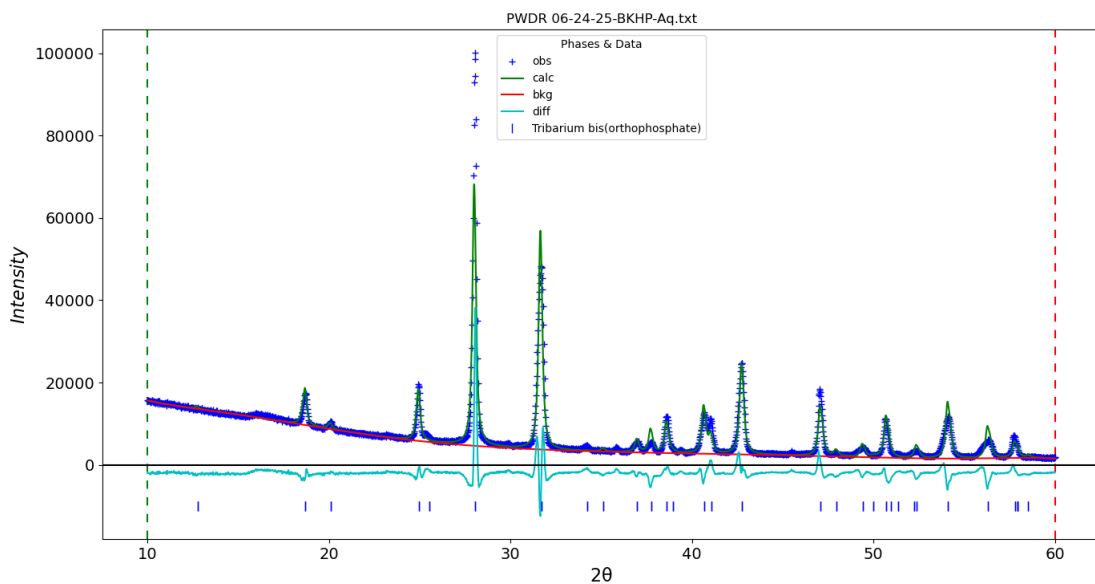


Figure 3: Pre-Milling

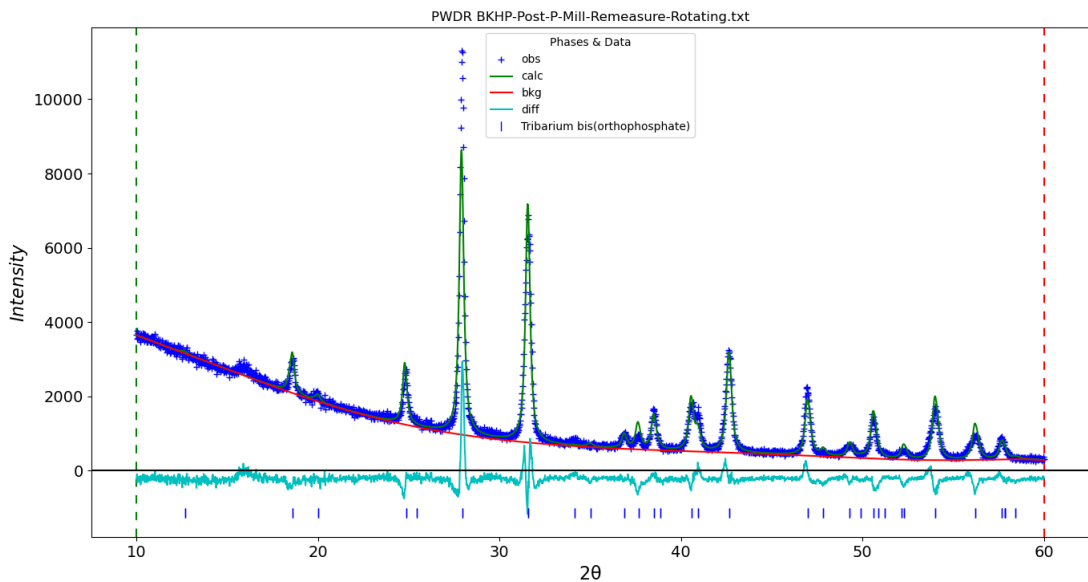


Figure 4: Post Planetary Milling

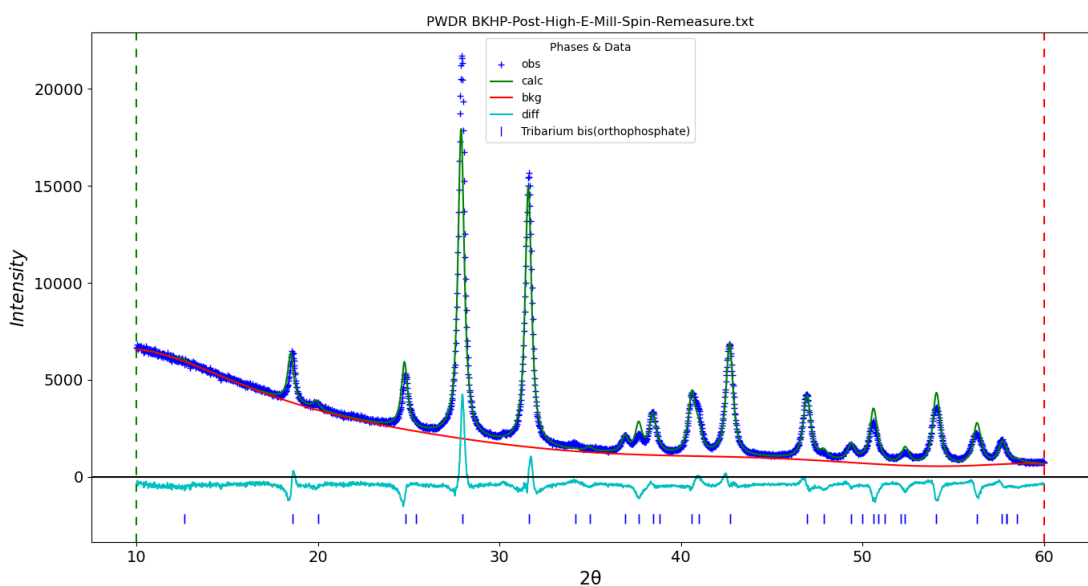


Figure 5: Post Planetary & High Energy Milling

2.1.2. Confocal Microscopy Results

The following samples were prepared for confocal microscopy all viewed on the 20x lens.

1. Pre-mill BKHP (there are two separate samples from each individual synthesis i.e., they were not combined as in for the diffraction pattern above)
2. Planetary Milled
3. Planetary & High Energy Milled

2.1.2.1. Pre-Mill

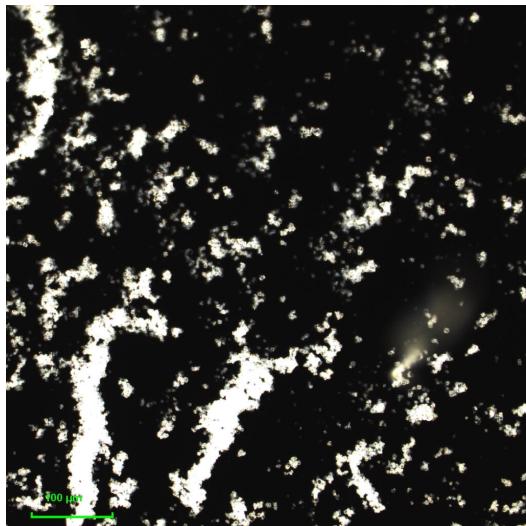


Figure 6: Pre-Mill Synthesis 1

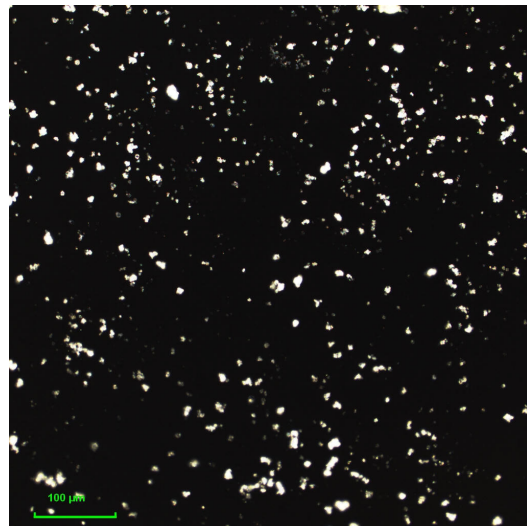


Figure 7: Pre-Mill Synthesis 2

2.1.2.2. Post Planetary Milling

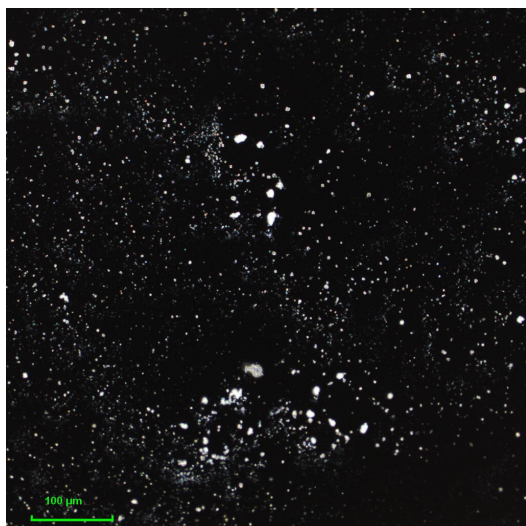


Figure 8: Post Planetary Mill

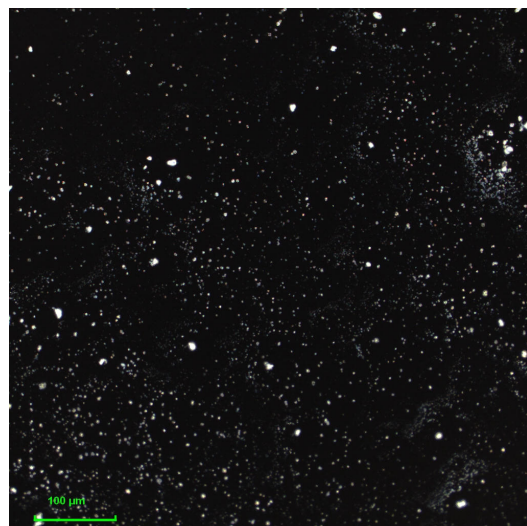


Figure 10: Post Planetary Mill

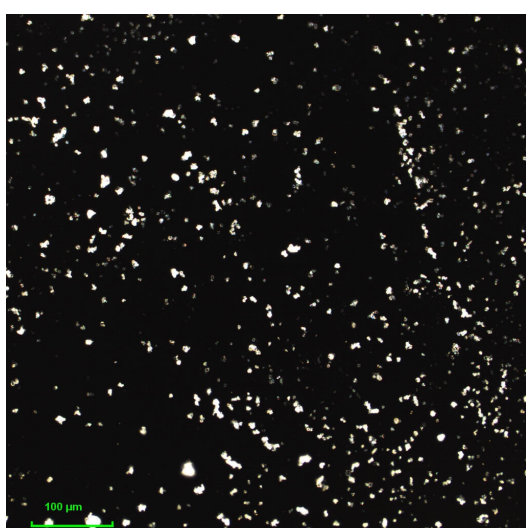


Figure 9: Post Planetary Mill

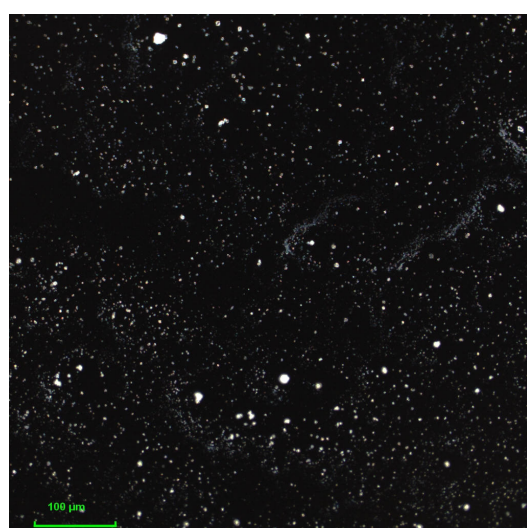


Figure 11: Post Planetary Mill

2.1.2.3. Post Planetary & High Energy Milling

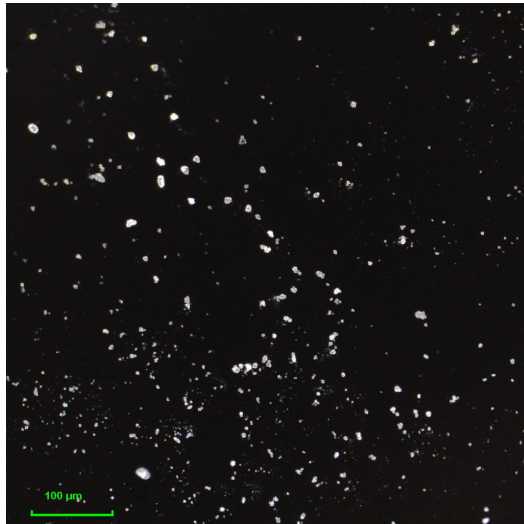


Figure 12: Post Planetary & High Energy Milling

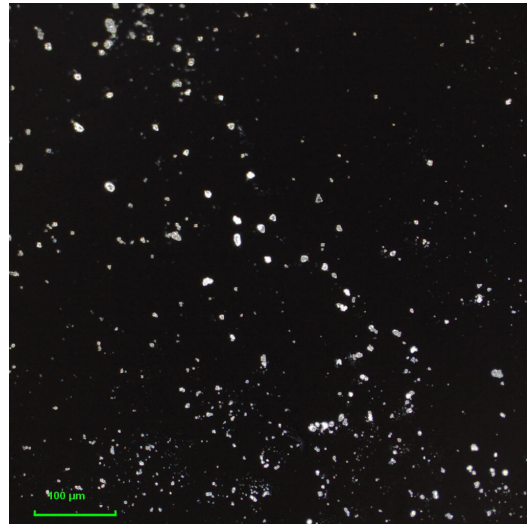


Figure 14: Post Planetary & High Energy Milling

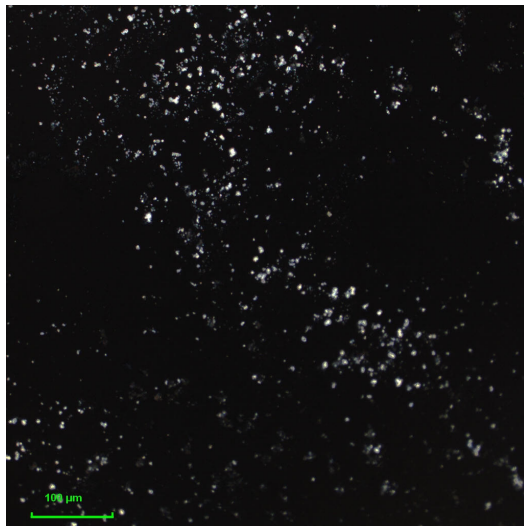


Figure 13: Post Planetary & High Energy Milling

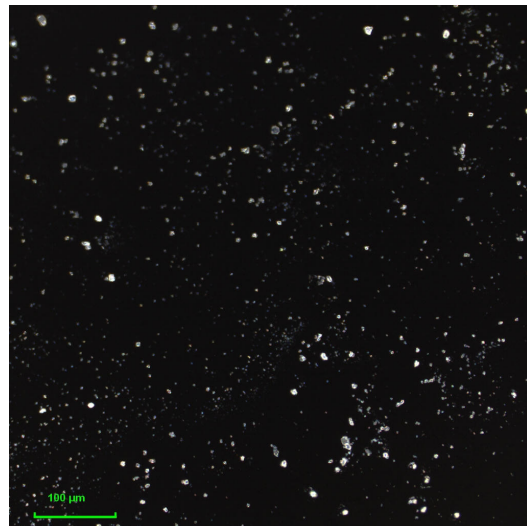


Figure 15: Post Planetary & High Energy Milling

2.1.2.4. Confocal Microscopy Comments

The confocal microscope is not a helpful tool in determining particle size because:

1. Depending on where in the sample the microscope is zoomed into, the distribution of particles vary wildly
2. Different parts of the solution have various concentration of particles, making samples on certain slides look further apart/closer together. This makes the qualitative judgement on particle size more difficult
3. Often difficult to distinguish between single particles and particles clusters
4. Microscope slides can have microscratches/other imperfections that may appear as long sludges or large blobs that protude both outwards/inwards of the slide (haven't resolved this)

Generally there doesn't seem to be any change pre/post-milling in the microscope images. The original paper cites crystal sizes as ranging from $0.2 - 2\mu\text{m}$. Measurements and images for single crystals were made/taken and ranged from $4 - 7\mu\text{m}$ shown below.

2.1.3. Dynamic Light Scattering Results

Attempted to use the Zetasizer machine in NUANCE for quantitative characterization of particle size and distribution. TLDR: DLS did not provide accurate data for a variety of reason, partially inherent to the instrument and poor sample preparation.

2.1.3.1. Sample Preparation

Assumed particle size of $2 - 3\mu\text{m}$, sonicated 0.035g of sample in 3.5mL of water for 2 hours and shaken every 30 minutes. Used refractive index as 1.648 and absorption as 0.001 (taken from ChatGPT as reasonable estimates)

2.1.3.2. Dynamic Light Scattering Comments

Instrument scientist Xinqi Chen believes the data to be of such poor quality therefore is not shown because:

1. Z-average values constantly fluctuate between multiple runs of the same sample
2. No intensity readings → concentration used too high
3. High polydispersity index values → no sharp peaks i.e., wide distribution of sizes

Issues stem from the non-stable suspension formed since BKHP concentration was likely too high. Regardless of if a stable suspension was formed at either a lower concentration or using a different solvent, multiple issues remain:

1. DLS can't distinguish clumped particles & single crystals
2. No guarantee "good" results (consistent Z-average values between runs) is representative of sample (i.e., larger clumps fall to bottom)
 - Is there crystal size reduction or big clumps broken up?

While DLS cannot resolve particles larger than $10\mu\text{m}$ if the aqueous synthesis did produce crystals of that size, single crystal conductivity measurements could be made.

With these factors in mind, a decision to not focus on characterizing particle/crystal size and distribution was made. Instead the focus was shifted to obtaining high conductivity values.

2.2. Making Pellets

All pellets are pressed at 5 tons for 5 minutes and 7 tons for 5 minutes. Material did not respond well to hot pressing. BKHP also deliquesces at ambient temperature.

$\text{Ba}_3(\text{PO}_4)_2$'s density taken from the Materials Project. BKHP x=1 density was calculated using $\rho = \frac{N_{\text{tot}} A_r}{V_{u.c} N_A}$ with $V_{u.c} = 586.5\text{\AA}^3$ and $N_{\text{tot}} = 3$ from the $\text{R}\bar{3}\text{m}$ space group

COMPOUNDS	DENSITY ($\frac{g}{cm^3}$)
BKHP $x=1$	4.29
$Ba_3(PO_4)_2$	5.17

Table 2: Barium Phosphate & $x = 1$ BKHP Densities

2.3. EIS Measurements

2.3.1. $100 \rightarrow 250^\circ C$ & Initial Ambient Measurement Pellets

SAMPLE	DENSITY ($\frac{g}{cm^3}$)	REL. DENSITY (%)	A/L (mm)
Planetary Milled	3.88	90.442	23.091
High Energy Milled	3.40	79.250	22.220

Table 3: Pellet Densities

Used $\rho = \frac{1}{R \frac{A}{L}}$ and converted to $\log(\sigma T) [\frac{S}{cm} K]$ used in the paper

2.3.2. $100 \rightarrow 250^\circ C$ Measurements

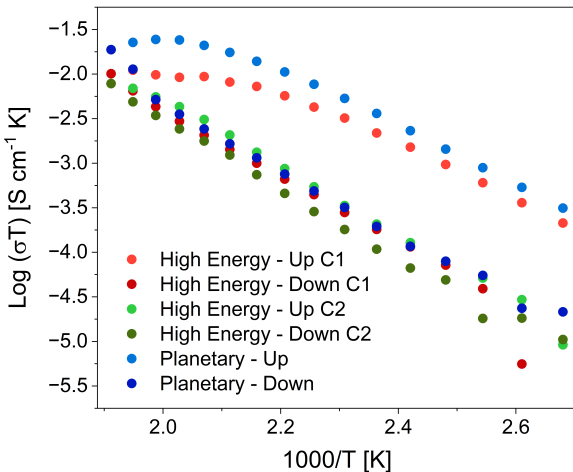


Figure 16: Arrhenius Plot

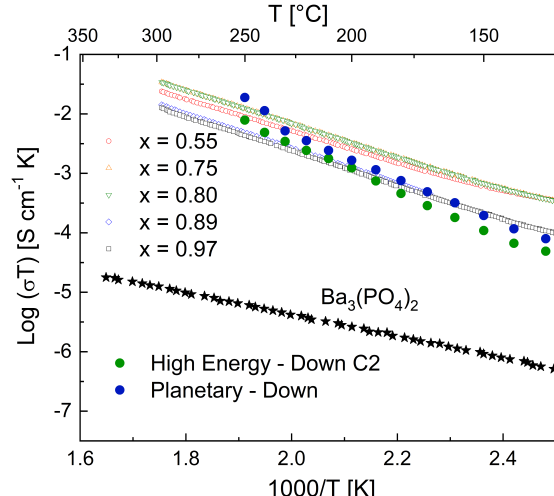


Figure 17: Arrhenius Plot rel. Paper

SAMPLE	EQUILIBRATION STEP (MIN)	MEASUREMENT STEP (MIN)
Planetary Milled	20	10
High Energy Milled	180	20

Table 4: Heating Profile $100 \rightarrow 250^\circ C$

- Both pellets heated in $10^\circ C$ increments
- Frequency range: 10^6 Hz \rightarrow 20 Hz

The initial ramp-up phase has a substantially higher conductivity than on either of the ramp down cycles. This suggest that the species are initially hydrated when the measurement is started at ambient temperature. This means that the most dry ramp down data points are used for comparison with values from the original paper. Figure 17 makes it clear that milling has no apparent impact on conductivity.

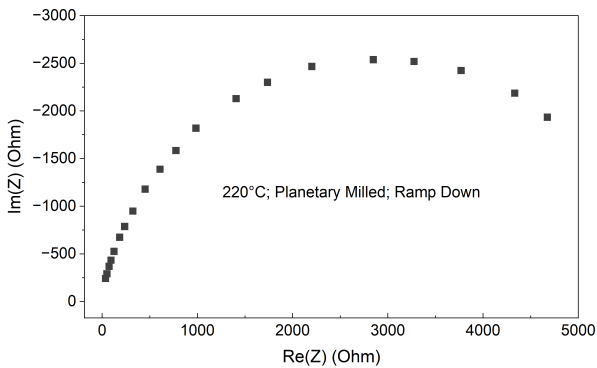


Figure 18: Single Arc at 220°C

Lower temperature measurements (i.e., 100°C) are prone to having more noise in the lower frequency range but all have the same general shape of a single arc.

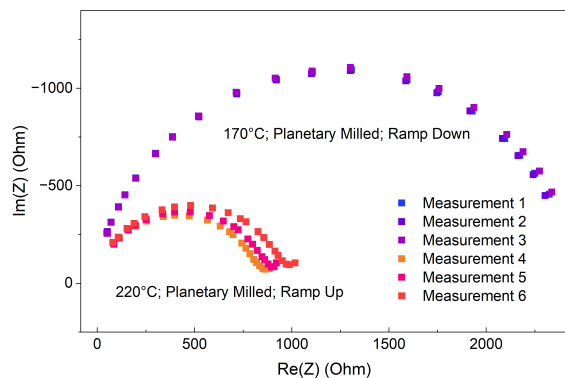


Figure 19: Planetary Milled Ramp Up Plot at 220°C & Ramp Down at 170°C

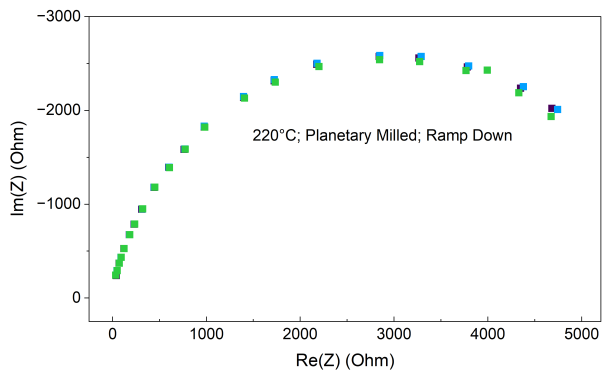


Figure 20: Planetary Milled Ramp Down Plot at 220°C

At elevated temperatures i.e., 220°C the 10 minute time between measurements is not enough to reach equilibrium while at lower temperatures it is. As expected from the arrhenius plot, the conductivity is lower at the same temperature in the ramp down compared to the ramp up.

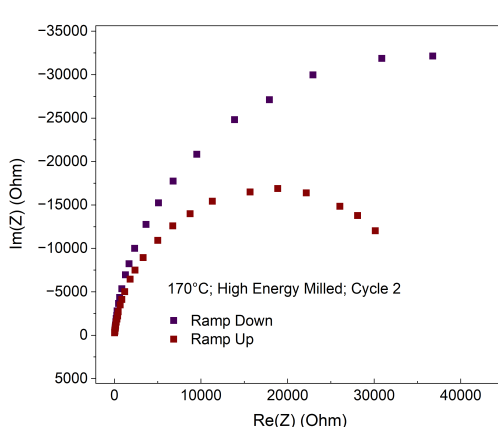


Figure 21: High Energy Milled Cycle 2 Plot at 170°C

The same cycle 1 behavior is observed for the high energy milled pellet.

Cycle 2 has higher temperature where arc fails to equilibrate (190°C v. 220°C) during ramp up.

Additionally the second cycle has a larger difference between the conductivity during ramp up and ramp down process also shown on the arrhenius plot and on the left.

2.3.2.1. Capacitance Analysis

VALUE	MEAN (F)	STDEV/MEAN (%)
QPE1-Q	3.64×10^{-10}	5.23
QPE1-n	0.916	2.51
Capacitance (F)	8.51696×10^{-10}	12.76

Table 5: Capacitance Values from 100 → 250°C Measurements

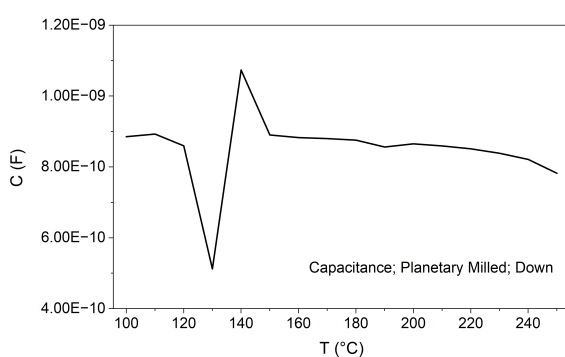


Figure 22: Planetary Milled Capacitance

Capacitance values are calculated from the most equilibrated QPE1-Q and QPE1-n values from the single arc RC-circuit fit. Capacitance values are calculated via the typical equation below:

$$QPE1-Q \times R^{1-QPE1-n}$$

As expected the chemical capacitance should not and did not vary drastically with temperature.

2.3.3. Ambient Measurements

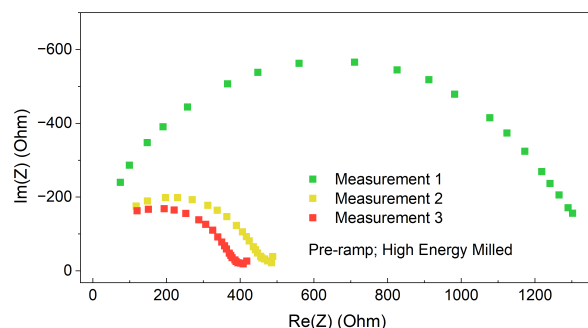


Figure 23: Pre-Ramp High Energy Milled

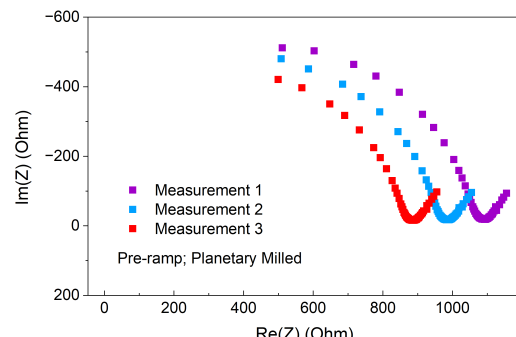


Figure 24: Pre-Ramp Planetary Milled

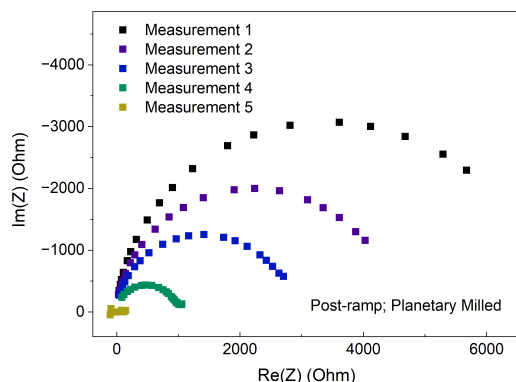


Figure 25: Post-Ramp Planetary Milled 1

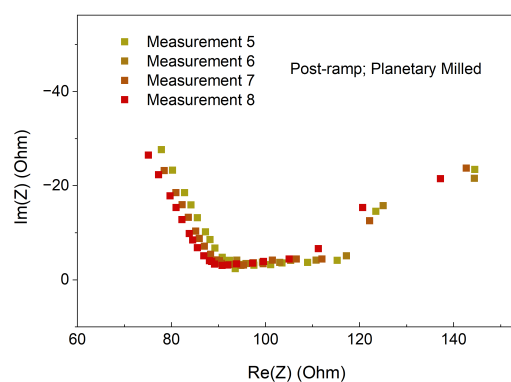


Figure 26: Post-Ramp Planetary Milled 2

Measurements taken under ambient conditions have shown to contain a tail (which could mark the start to a second arc) and to be prone to a high amount of hydration. None of the measurements shown above were fully equilibrated.

The tail could be either an electrode response or signal that there exists both a highly conductive bulk arc and a less conductive grain boundary arc which is what is shown at elevated temperatures. To determine which response is shown, intermediate temperature measurements from ambient temperature to 100°C was made.

To better understand the hydration behavior of BKHP, measurements were made to visualize the conductivity & nyquist plot of fully equilibrated BKHP at ambient temperatures. Additionally TGA & DSC data was collected.

2.3.4. TGA & DSC Data

Minimal analysis was conducted for the TGA & DSC data. There is relative confidence that the sample used for analysis was the high energy milled powder. This is of note because the corresponding EIS measurements made at 125°C appeared to fully equilibrate but was made from the ball mill synthesis method's BKHP which does not likely have substantial potassium incorporation (i.e., the ball mill synthesis did not produce BKHP.) Therefore the data has been omitted below.

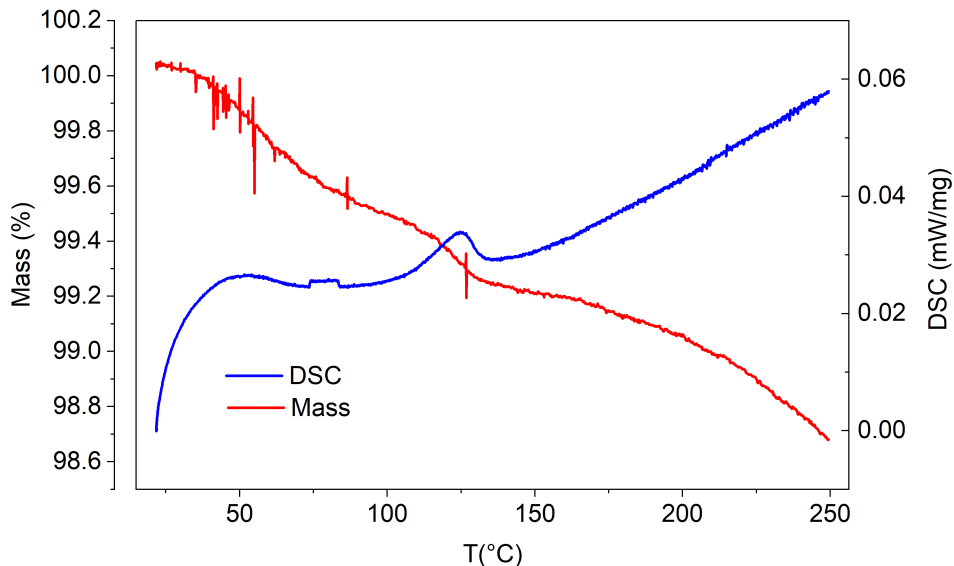


Figure 27: TGA & DSC Data using High Energy Milled Powder

2.3.5. Ambient Hydration Behavior & Intermediate Temperature Pellets

SAMPLE	DENSITY ($\frac{\text{g}}{\text{cm}^3}$)	REL. DENSITY (%)	A/L (mm)
Unmilled	3.63	84.6	19.356
Planetary Milled	3.68	85.7	14.92

Table 6: Unmilled & Planetary Milled V2 Pellet Densities

2.3.6. Ambient Hydration Behavior

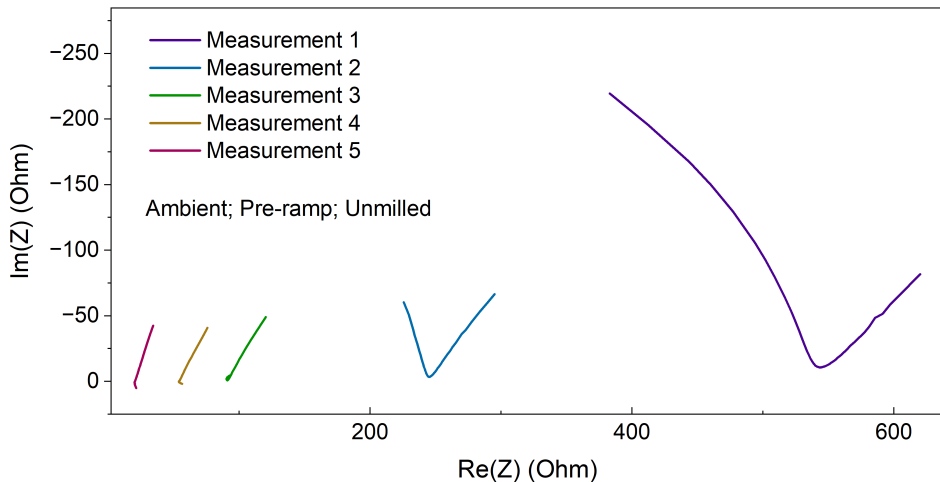


Figure 28: Ambient Equilibration Measurement on Unmilled BKHP

The sample was allowed to equilibrate overnight. Measurement 5 is on the order of 2Ω which signifies that BKHP is prone to a high degree of hydration. Even after the overnight measurement, there still seems to be some degree of fluctuation in the measurement.

Hydrated BKHP from measurement 5 shown above is approximately on the same order of magnitude as CsH_2PO_4 at 240°C .

SAMPLE	$\rho(\frac{\text{S}}{\text{cm}})$	$\log(\sigma T)[\frac{\text{S}}{\text{cm K}}]$
BKHP	2.6×10^{-3}	-0.1177
CDP	5.0×10^{-2}	1.42

Table 7: BKHP v. CDP Conductivity

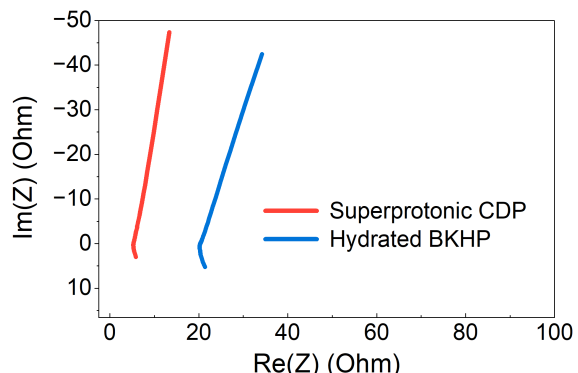


Figure 29: 250°C CDP v. Hydrated BKHP

Since the relative size of the tail is constant during equilibration and resembles the electrode response in superprotonic CDP, it is possible that the tail seen in ambient measurements is also an electrode response.

Additionally, since the 5Ω offset is taken as the resistance for the system's conductivity, it will be important to observe if a similar offset exists in all EIS measurements as it could signal the bulk + grain boundary resistance. This offset is the preliminary theory from Prof. Haile surrounding the bulk conductivity. It is challenging to confirm this theory since the lower frequency data points at elevated temperatures rarely start at $Z'' = 0$.

2.3.7. Intermediate Temperature Measurements

SAMPLE	EQUILIBRATION STEP (MIN)	MEASUREMENT STEP (MIN)
Unmilled & Planetary	180	2

Table 8: Heating Profile 100 → 250°C

- Both pellets heated in 10°C increments
- Frequency range: 10⁶ Hz → 20 Hz

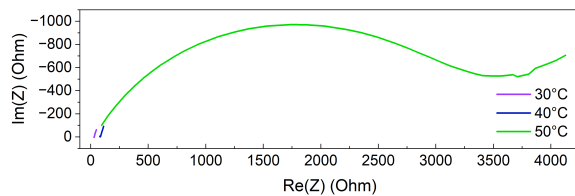


Figure 30: 30°C to 50°C Unmilled

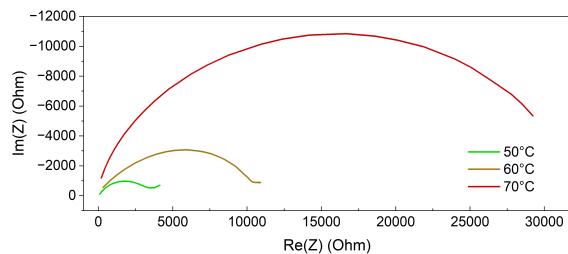


Figure 31: 50°C to 70°C Unmilled

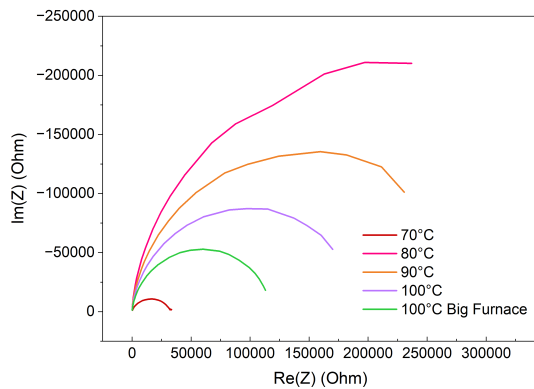


Figure 32: 70 to 100°C Unmilled

- Measurements shown are spaced 3 hours apart

As expected when initially heating the sample, the material is less conductive since the sample is dehydrating even though conductivity increases with temperature.

At the 70°C to 80°C, conductivity increases with an increase in temperature, signifying that temperature plays a larger role than hydration in determining conductivity.

Either the measurement has not equilibrated after 3 hours since the 100°C measurement in the big furnace is more conductive than that of the box furnace or the temperature in the box furnace is inaccurate (which is definitely possible.) Planetary milled pellet's intermediate temperature measurements are shown below.

2.3.8. Intermediate Temperature Transition

Quite noticeably, there is a large jump between 40°C and 50°C. The following measurements were made to characterize the evolution in such a jump. The measurements are taken roughly 2 minutes apart and are concentrated in the initial ramp up phase from 40°C to 50°C.

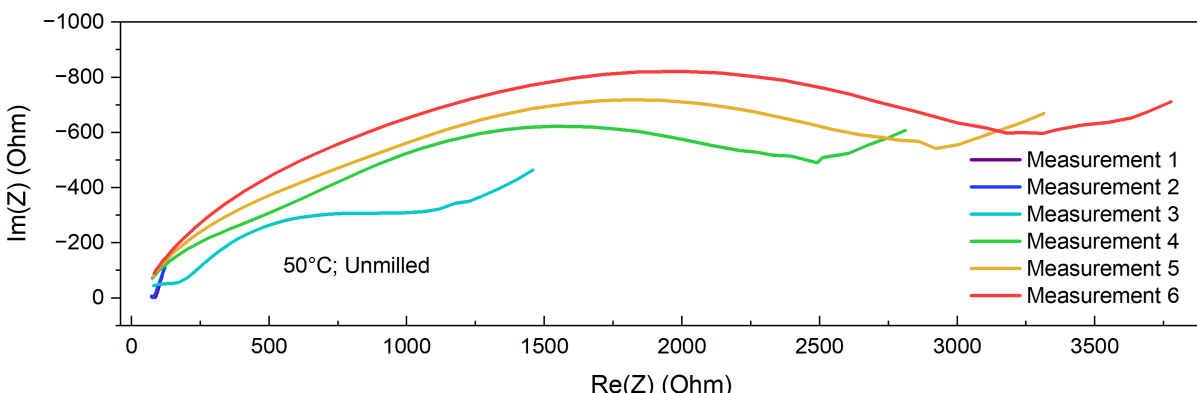


Figure 33: Unmilled 50°C Evolution

The broad arcs and the double arcs visible in measurement 3 may suggest that under most measurement conditions there is an overlap between the grain boundary and bulk arcs.

Measurement 3 from the unmilled sample is of particular interest. It is unclear as to why this behavior is only captured in the unmilled sample and not in the planetary sample. If it is the case that the evolution occurs so quickly as to be a rare coincident that it was captured in the unmilled sample, it is also possible that the sample undergoes an evolution during the minute long measurement itself i.e., the two arcs shown are instead a single arc shifting.

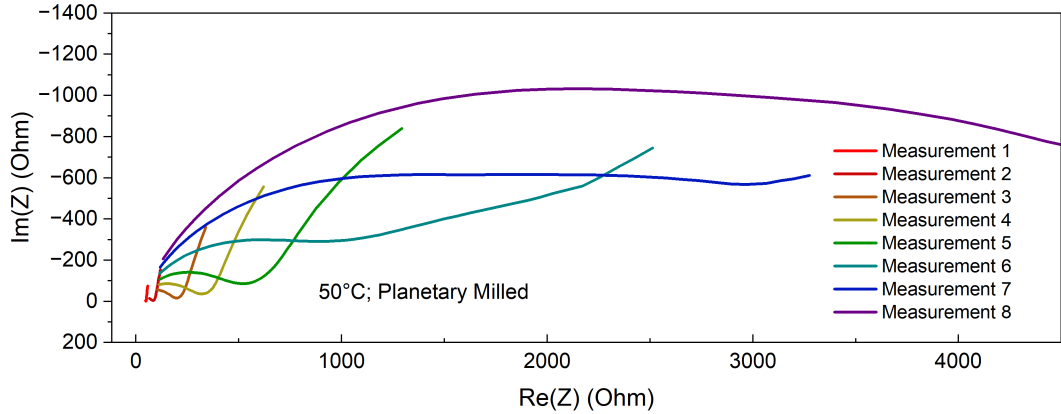


Figure 34: Planetary Milled 50°C Evolution

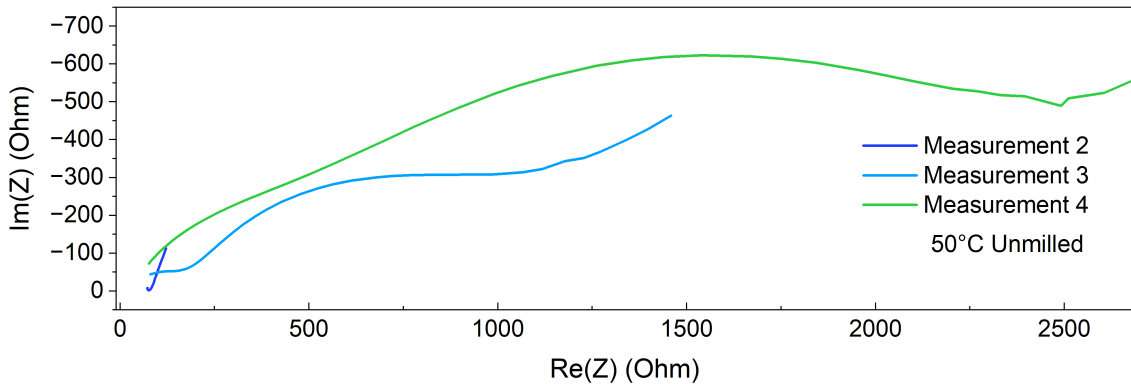


Figure 35: 50°C Evolution Close-Up

ARC	RESISTANCE(Ω)	$\sigma(\frac{\text{S}}{\text{cm}})$	$\log (\sigma T)[\frac{\text{S}}{\text{cm}} \text{K}]$
1st	295.8	1.75×10^{-4}	-1.00273
2nd	1232	4.19×10^{-5}	-1.19984

Table 9: First & Second Arc Conductivity

Both arcs in measurement 3 were fitted with a typical single arc equivalent circuit. An attempt was made to use the capacitance and resistance values from the single arc equivalent circuit fits to fit a double arc equivalent circuit but it was not successful. This meant that extrapolating the separate arc values to different temperatures was not successful.

ARC	QPE1-Q	QPE1-N	CAPACITANCE (F)	DIELECTRIC CONSTANT
1st	3.13×10^{-24}	0.43649	5.50×10^{-11}	32.11

ARC	QPE1-Q	QPE1-N	CAPACITANCE (F)	DIELECTRIC CONSTANT
2nd	9.94×10^{-13}	0.60675	5.22×10^{-8}	30439.76

Table 10: First & Second Arc Fit Results

The capacitance is calculated via the equation referenced above. The dielectric constant was calculated via: $\epsilon = \frac{CL}{\epsilon_0 A}$ where:

ϵ_0	$8.8541878 \times 10^{-12} \left(\frac{F}{m} \right)$
C	Capacitance
A	Pellet Area
L	Pellet Thickness

Table 11: Dielectric Constant Equation

The dielectric constant of the first arc is in the range of 30 – 100 which corresponds to a value typical of the bulk arc. The dielectric constant of the second arc is not within a reasonable range suggesting that it is not the bulk behavior.

It is also possible that given BKHP is an anisotropic material, the messy intermediate temperature arcs are a combination of the bulk, grain boundary, and the electrode responses.

2.3.9. Bode Plot Comments

It is challenging to use the bode plot to determine if there exists an offset suggesting a bulk arc. Many measurements do not approach $Z'' = 0$ and the ones that do have no plateau in the bode plot in the higher frequencies which is due to our limited measurement conditions.

2.4. Humid Measurements

It is likely that the bulk conductivity does not change with humidity. Therefore regardless of if the arc seen in the majority of the EIS measurements are associated with the grain boundary or the bulk response, the resistance/conductivity under humid conditions set a lower bound to the system's conductivity. While there exists a tail in most of the nyquist plots since it does not change with temperature, evidence supports it is not an arc rather an electrode response.

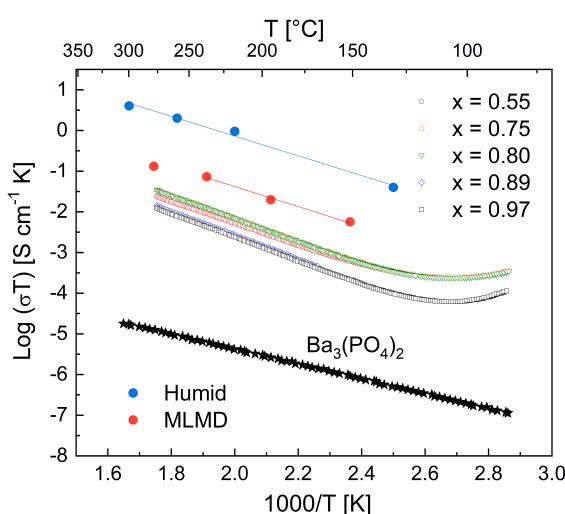


Figure 36: Humid Arrhenius Plot

Measurements were made under humid conditions of 68.84kPa. The last measurement at 300°C did not equilibrate due to an measurement error; therefore it is likely an underestimation of the true conductivity.

As shown, the sample's total conductivity is significantly higher under humidity than under dry conditions. Therefore it is shown that the material's conductivity is at least around 5-6x greater than initially measured. Still, our measurements remain a little more than an order of magnitude less than predicted by the computational results from the group's collaborators.

Varying humidities were tested at 150°C. It is shown below that from 37.48kPa to 68.94kPa the system's conductivity increases but decreases from 83.54kPa onwards.

HUMIDITY (kPa)	RESISTANCE (Ω)	$\sigma(\frac{S}{cm})$	$\log(\sigma T)[\frac{S}{cm}K]$
37.48	8249	6.26×10^{-6}	-2.71
68.94	1236	4.18×10^{-5}	-1.84
83.54	4405	1.17×10^{-5}	-2.38

Table 12: 150°C Humidity Measurements

As shown the behavior of the system over time resembles that of hydration under ambient conditions with the exception that despite the substantially higher vapor pressure and humidity, the sample does not exhibit the equilibrated behavior at ambient conditions.

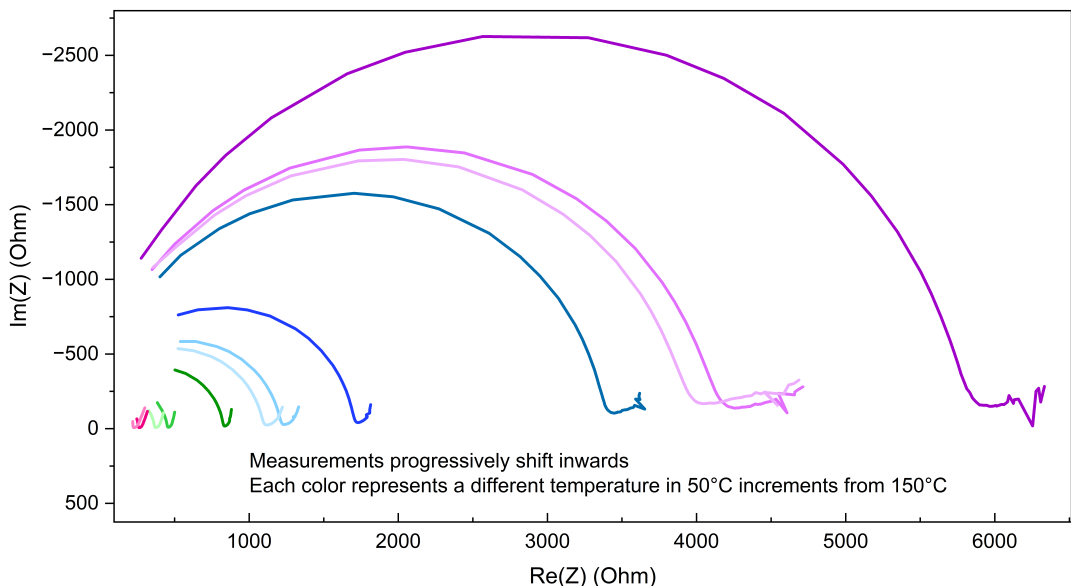


Figure 37: 200°C BKHP at 68.94 kPa

Additionally the measurement tends to settle to a more conductive system relatively quickly and gradually drift to become more resistive as shown below.

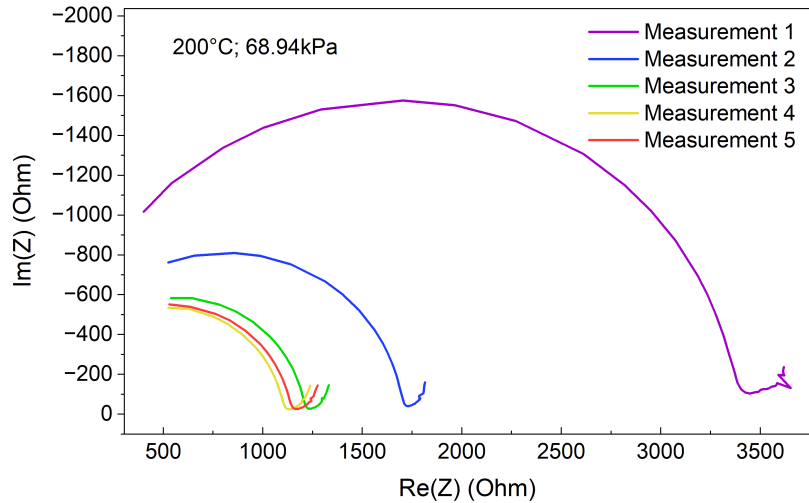


Figure 38: 200°C BKHP at 68.94 kPa

2.5. Future Work

Since it is shown that BKHP's true conductivity is at least nearly an order of magnitude higher than what was originally measured without optimizing humidity conditions, it is almost certain there is more work to be done to probe the material's true conductivity. Additional experiments such as introducing a bias to the system could be made.

3. Ball Mill Synthesis

3.1. Mill Synthesis Preparation

3.1.1. Synthesis Mechanism

The proposed synthesis mechanism is shown again below:



The secondary potassium phase $\text{K}_3\text{H}_3(\text{PO}_4)_2$ is not shown to be stable which explains the use of the two other potassium precursor phases.

- 1:1 molar ratio of KH_2PO_4 : $\text{K}_2\text{HPO}_4 = \text{K}_3\text{H}_3(\text{PO}_4)_2$
- 2:1 molar ratio of $\text{Ba}_3(\text{PO}_4)_2$: $\text{KH}_2\text{PO}_4 + \text{K}_2\text{HPO}_4 \rightarrow \text{Ba}_6\text{K}_3\text{H}_3(\text{PO}_4)_2$

Aiming for around 2.5g of sample per synthesis:

COMPOUNDS	MASS (g)	MOL
$\text{Ba}_3(\text{PO}_4)_2$	1.9877	3.3022×10^{-3}
K_2HPO_4	0.28762	1.6511×10^{-3}
KH_2PO_4	0.22469	1.6511×10^{-3}

Table 13: Precursor Mass for 2.5g of $x = 1$ BKHP

3.1.2. Synthesis Setup

Since the K_2HPO_4 & KH_2PO_4 precursor phases are water soluble, an upper bound for the potassium phase incorporation is first made i.e., the hypothetical stoichiometry where potassium phases are visible post milling. A corresponding lower bound will also be established i.e., phase pure post milling.

Diffraction data is collected prior to milling, after milling, and post-washing where the water soluble potassium phases are removed.

The upper bound of potassium incorporation can be used to determine the potassium occupancy via diffraction. Corresponding conductivity and proton NMR measurements were also made..

3.1.3. $\text{Ba}_3(\text{PO}_4)_2$ Impurity Phase

Before milling, the bottled $\text{Ba}_3(\text{PO}_4)_2$ was analyzed. There exists an barium hydroxyapatite $\text{Ba}_5(\text{PO}_4)_3\text{OH}$ impurity phase (4.2% weight fraction & 3.811% phase fraction.)

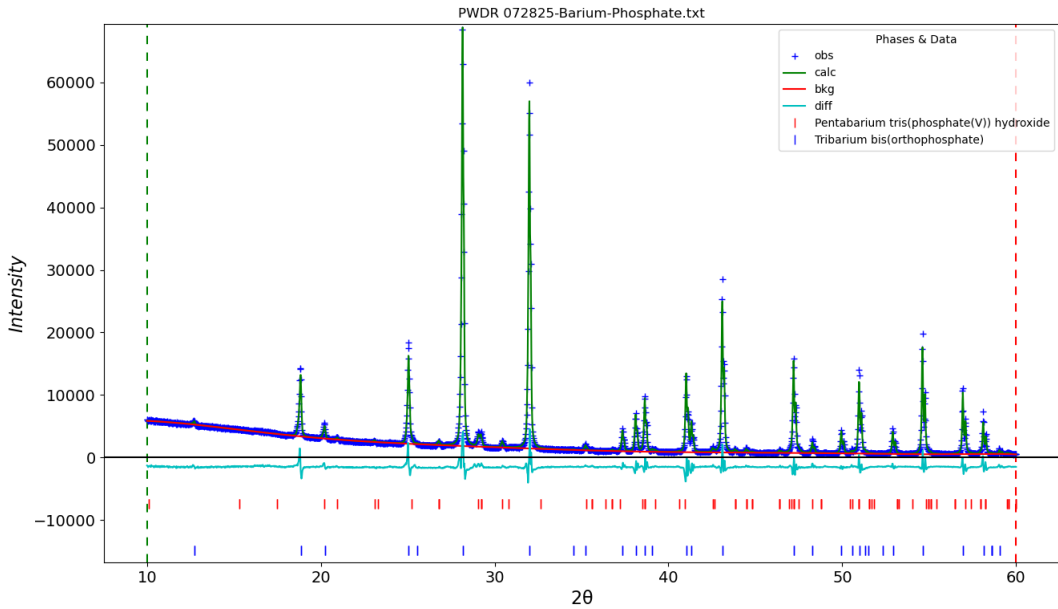


Figure 39: PXRD for Bottled $\text{Ba}_3(\text{PO}_4)_2$

An $x = 1$ synthesis was completed during Spring 2025 where the sample appeared phase pure after 3.5 hours in the high energy mill. Washing did not remove the impurity peaks but milling $\text{Ba}_3(\text{PO}_4)_2$ with the impurity phase alone did lead to a phase pure sample.

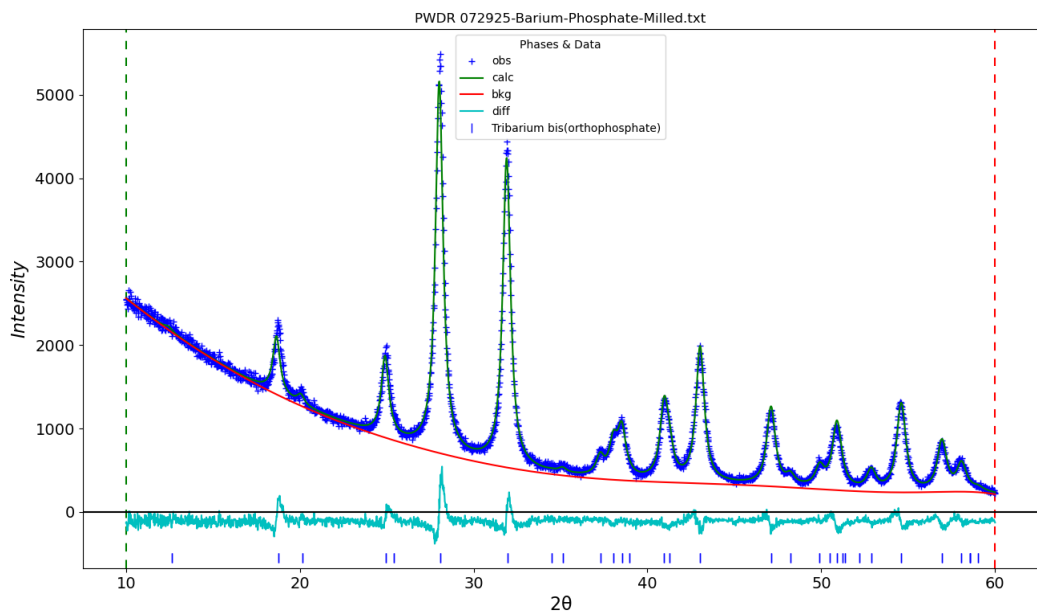


Figure 40: PXRD for Bottled $\text{Ba}_3(\text{PO}_4)_2$ Post-Milling

It may be possible that the impurity phase (known to be mechanically ductile) becomes amorphous after milling but no experiments have been made to directly confirm this.

Since the impurity phase is no longer visible after milling and relatively minor, the bottled $\text{Ba}_3(\text{PO}_4)_2$ was used in subsequent experiments. To ensure the impurity peaks are no longer visible when the pre-cursors are combined, 12g $\text{Ba}_3(\text{PO}_4)_2$ was milled for 5 hours & 10 minutes where impurity phase has minor 0.5% weight fraction and 0.4% phase fraction.

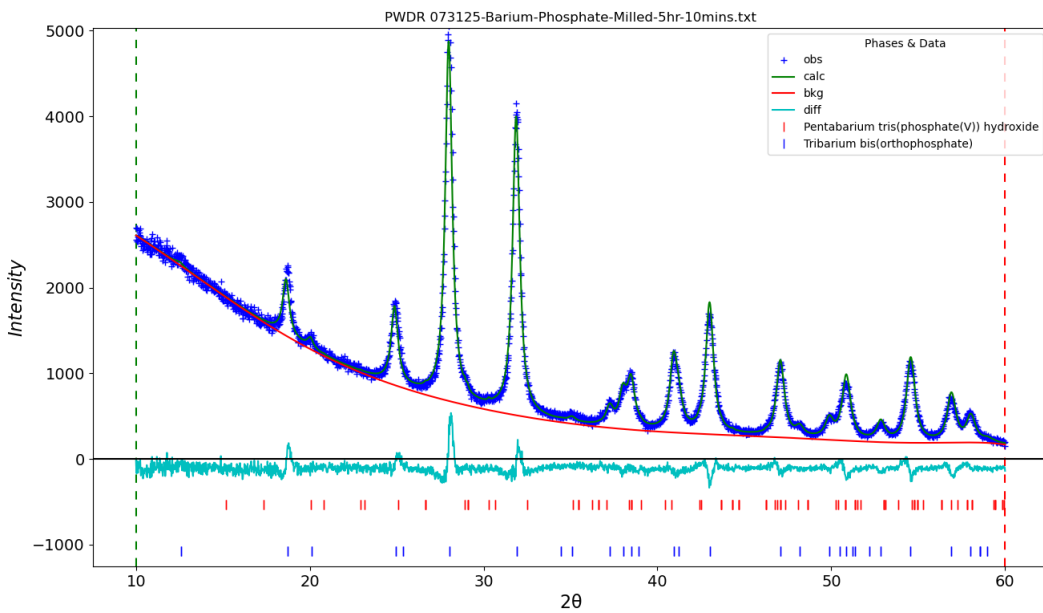


Figure 41: PXRD for Bottled $\text{Ba}_3(\text{PO}_4)_2$ Post 5 Hours & 10 Minutes Milling

3.1.4. Steel Impurities

Since the samples were milled using the steel container and jar, there is contamination in the powder which has a visual color difference post-milling. Since the steel impurity was not visible in the diffractometer, the high energy milled was used for all subsequent experiments

3.2. Determining Potassium Detection Limit

3.2.1. $x = 1$ Synthesis Replication

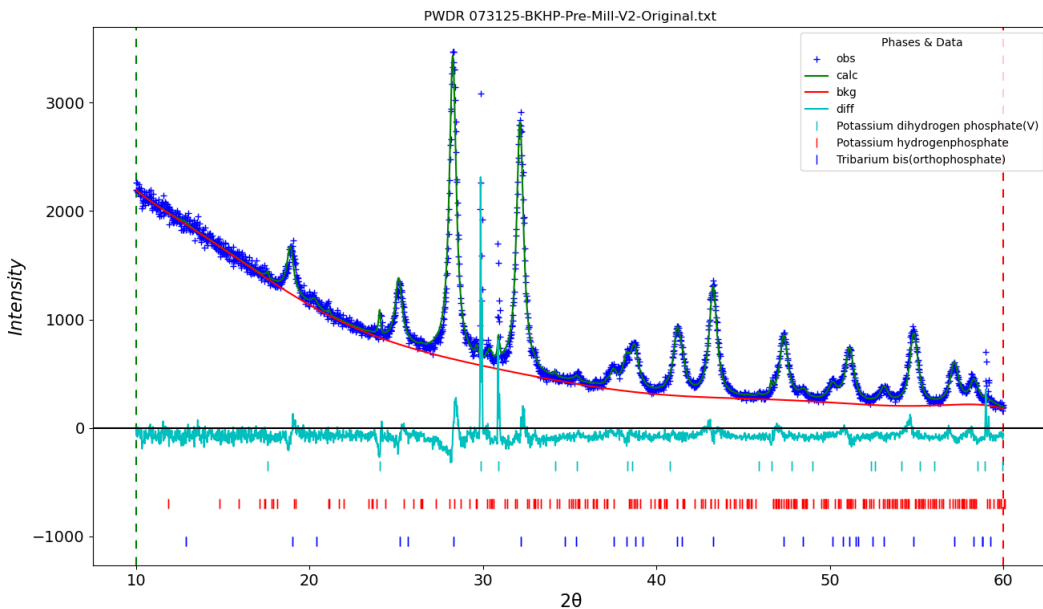


Figure 42: PXRD Data for $x = 1$ Synthesis Pre-Mill

COMPOUND	ACTUAL MASS (G)	THEORETICAL MASS (G)
K_2HPO_4	0.2824	0.28762
KH_2PO_4	0.2220	0.22469
$Ba_3(PO_4)_2$	1.9859	1.9877

Table 14: $x = 1$ synthesis measurements

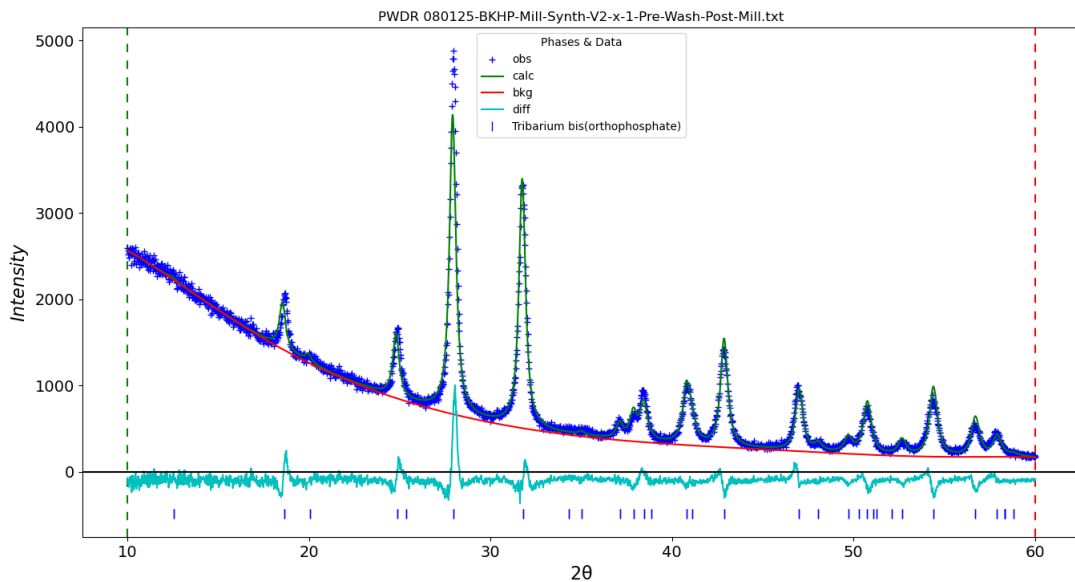


Figure 43: PXRD Data for $x = 1$ Synthesis Pre-Wash & Post-Mill

Sample appears phase pure after milling and prior to washing serving as the lower bound.

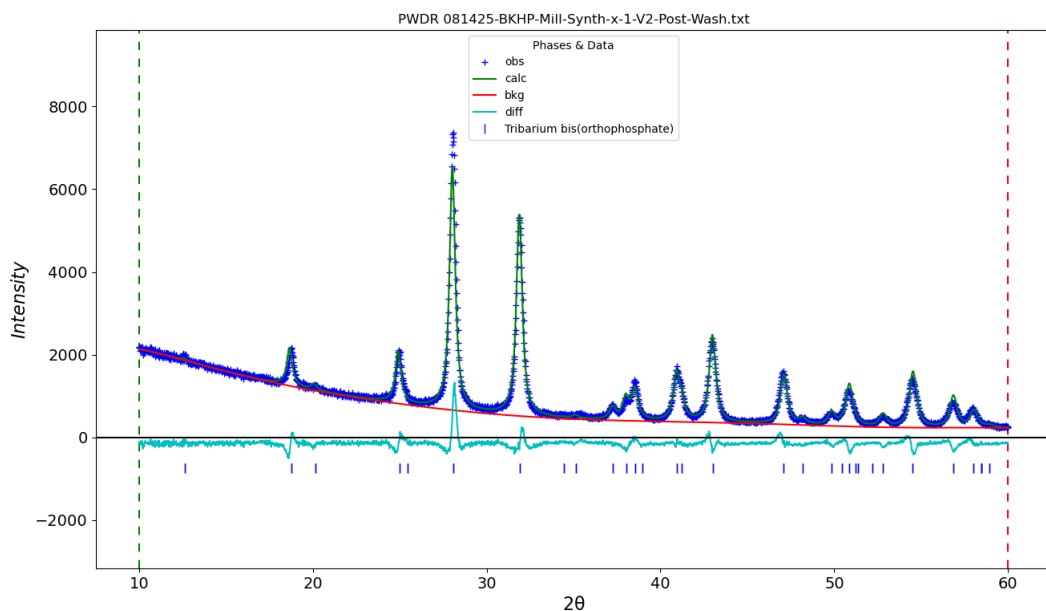


Figure 44: PXRD Data for $x = 1$ Synthesis Post-Wash

3.2.2. $x = 2$ Synthesis

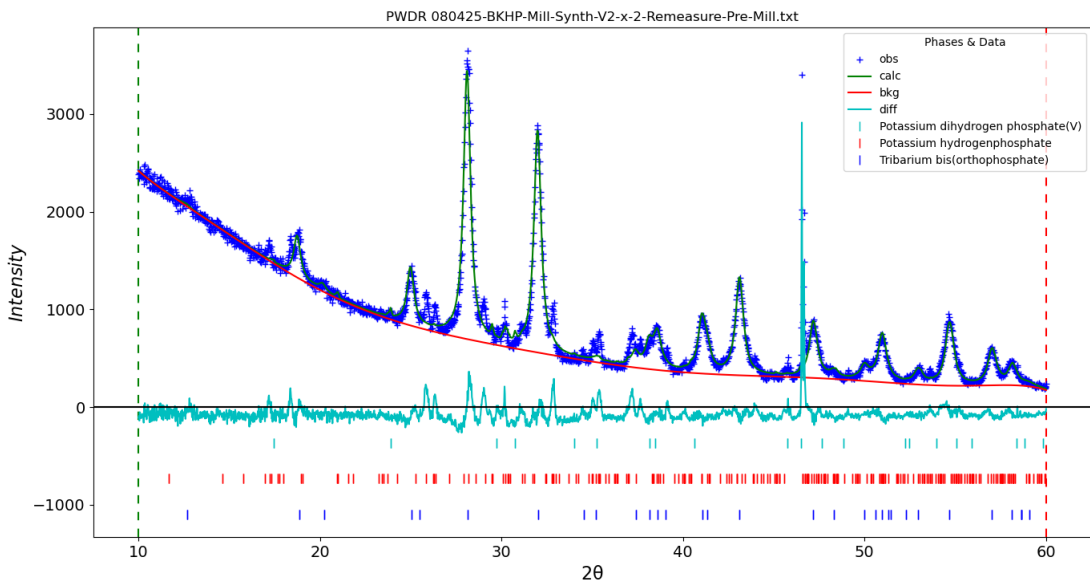


Figure 45: PXRD Data for $x = 2$ Synthesis Pre-Mill

COMPOUND	ACTUAL MASS (G)	THEORETICAL MASS (G)
K_2HPO_4	0.5727	0.57524
KH_2PO_4	0.4476	0.44938
$\text{Ba}_3(\text{PO}_4)_2$	1.9860	1.9877

Table 15: $x = 2$ Synthesis Measurements

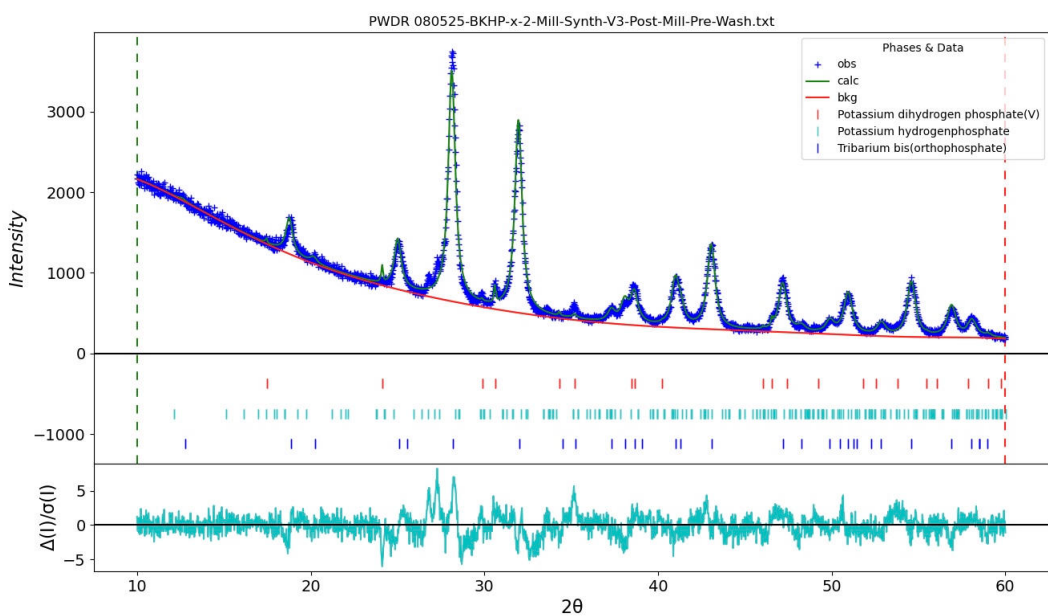


Figure 46: PXRD Data for $x = 2$ Synthesis Post-Mill/Pre-Wash

Clearly exists residual potassium phases after milling and prior to washing therefore serves as upper bound for potassium occupancy refinement.

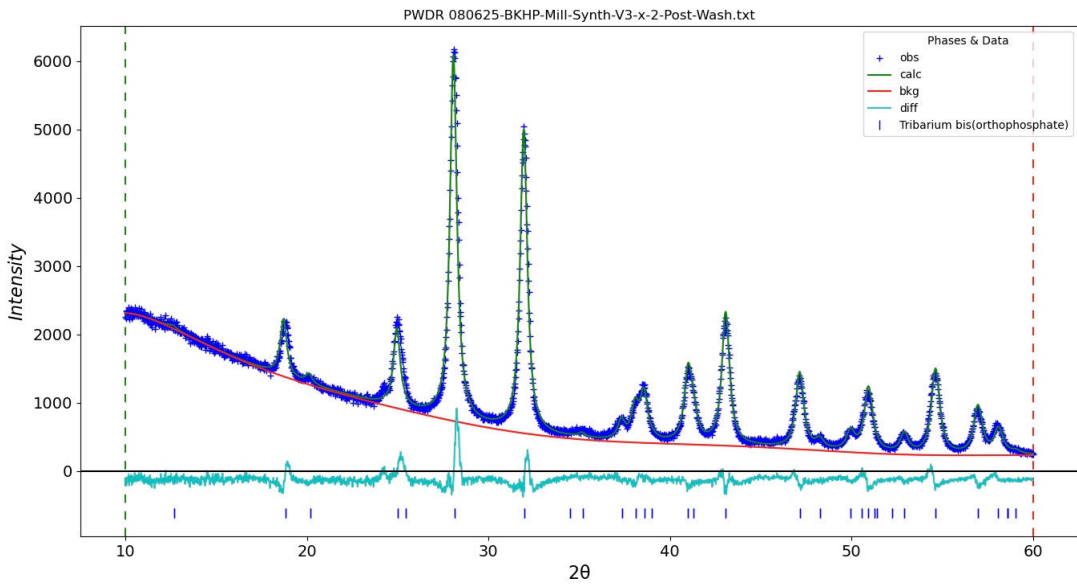


Figure 47: PXRD Data for $x = 2$ Synthesis Post-Wash

There exists a few residual peaks after washing. The sample was re-washed with silicon powder as a reference for the sample displacement in a long scan. The long scan did not show the shoulder near 25° or the fluctuations in the background scan. The pattern above is the only phase pure diffraction pattern collected.

3.3. Characterizing Washed $x = 2$ Sample

3.3.1. Potassium Occupancy Refinement

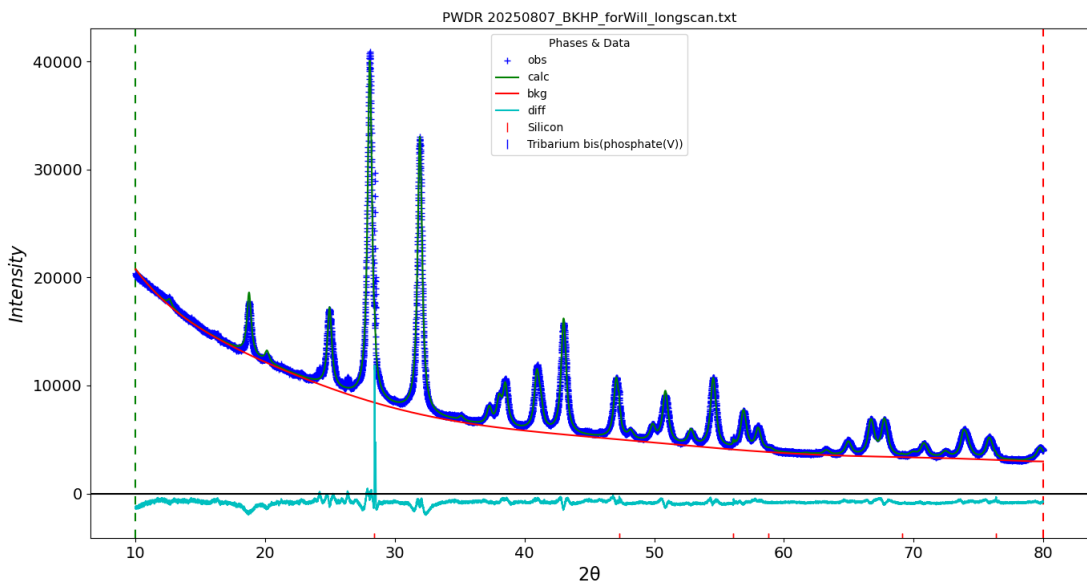


Figure 48: PXRD Data for Failed Potassium Occupancy Refinement with Silicon

Gordon helped perform the potassium occupancy refinement and the diffraction scan on the SmartLab instrument as opposed to the Ultima which all previous diffraction patterns were measured on.

The potassium occupancy refinement failed as the occupancy did not converge. On the other hand a sample aqueous synthesis diffraction pattern successfully converged to a value.

3.3.2. Lattice Parameter Analysis

x_{Total}	$a(\text{\AA})$	$c(\text{\AA})$
0.51	5.6209	21.114
0.59	5.6266	21.120
0.70	5.6304	21.138
0.80	5.6359	21.151
0.85	5.6421	21.139
0.94	5.6532	21.130
1.01	5.6640	21.110

Table 16: Lattice Parameters from Chrisholm et. al

The lattice parameters derived from the diffraction refinements do not align with the values from Chrisholm et. al.

It was shown that there is significant deviation in lattice parameters with/without silicon as a sample displacement reference.

SAMPLE	$a(\text{\AA})$	$c(\text{\AA})$
$\text{Ba}_3(\text{PO}_4)_2$	5.5969	21.00815
$x = 1$	5.60904	21.01913
$x = 2$	5.6051	21.02864

Table 17: Lattice Parameters from Post-Wash Milled Synthesis

While the results are not conclusive as these samples do not use silicon, at a glance it does not support that BKHP was synthesized via the ball mill.

3.3.3. Proton Nuclear Magnetic Resonance Spectroscopy

Non-quantitative proton NMR was conducted on the $x = 2$ washed milled synthesis sample and a traditional aqueous synthesis sample for reference.

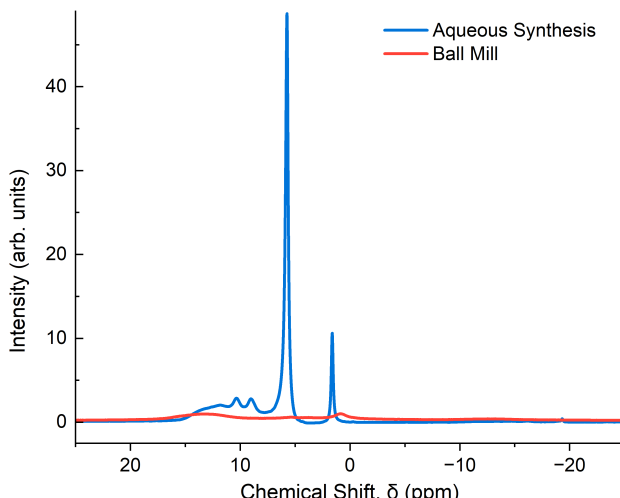


Figure 49: Proton NMR Plot of Aqueous v. Ball Mill Synthesis BKHP

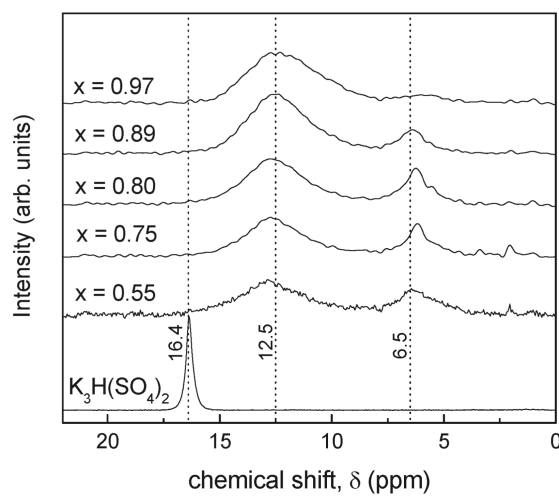


Figure 50: Proton NMR Plot from Chrisholm et. al

Measurements were made within an hour of each other in the same magnetic field, using the same pulse program, and using similar sample masses.

There is a significant difference between the intensities of the aqueous synthesis and the ball mill synthesis NMR results. While the relative values of the intensities cannot be directly referenced for potassium incorporation as a non quantitative measurement was performed, the substantial difference suggests that the ball mill synthesis has significantly less, if no potassium incorporation relative to the $x \approx 1$ aqueous synthesis.

The correlation between proton and potassium incorporation is derived from the crystallographic structure of the material where each proton substitutional site corresponds to a potassium substitutional site.

Since the $x = 1$ sample appears phase pure in the diffraction pattern after milling/prior to washing and considering the minimal potassium incorporation, it is confusing as to where the extra potassium is going.

3.3.4. Washing for Potassium

The rinsed solution of an $x = 1$ mill synthesis sample was saved and analyzed. Since the sample appeared phase pure in the diffraction pattern, ideally washing would not contain any potassium ions which signals potassium incorporation into the $\text{Ba}_3(\text{PO}_4)_2$ lattice.

To determine if potassium is in the washed solution, $\text{Na}(\text{C}_6\text{H}_5)_4\text{B}$ was used. 5 drops of the unknown solution was centrifuged with 5 drops of 3M NaOH. Complete precipitation was confirmed with one more drop of NaOH. If there exists potassium ions in the solution a white precipitate forms immediately when 2 drops of 0.005M $\text{Na}(\text{C}_6\text{H}_5)_4\text{B}$ is added.

The washed solution did form a precipitate signaling potassium. Soluble barium and potassium phases were also subjected to the test to confirm the validity of the test.

WASHED $x = 1$ SOLUTION	FORMED PRECIPITATE	HAS K^+
K_2HPO_4 Solution	Formed Precipitate	Has K^+
$\text{Ba}(\text{OH})_2$ Solution	Did not Precipitate	No K^+

Table 18: K^+ Ion Test Results

3.3.5. $x = 1$ Milled Synthesis Pellet

A pellet was made using powder from an $x = 1$ milled synthesis. The sample was only heated on a single ramp up cycle from 100°C to 250°C due to a error in the furnace.

SAMPLE	DENSITY ($\frac{\text{g}}{\text{cm}^3}$)	REL. DENSITY (%)	A/L (mm)
Milled Synthesis	4.18	97.4	17.18

Table 19: Milled Synthesis Pellet Density

SAMPLE	EQUILIBRATION STEP (MIN)	MEASUREMENT STEP (MIN)
Milled Synthesis	180	20

Table 20: Milled Synthesis Heating Profile 100 → 250°C

The milled synthesis conductivity is substantially higher than that of $\text{Ba}_3(\text{PO}_4)_2$ as shown below but is still lower than the aqueous synthesis BKHP. Since the other measurements in the arrhenius plot are from ramp down measurements, the other samples shown are substantially less hydrated than that of the milled synthesis measurement. This means that the milled synthesis conductivity is an overestimation of the conductivity as shown in the other cycled arrhenius plot to the left.

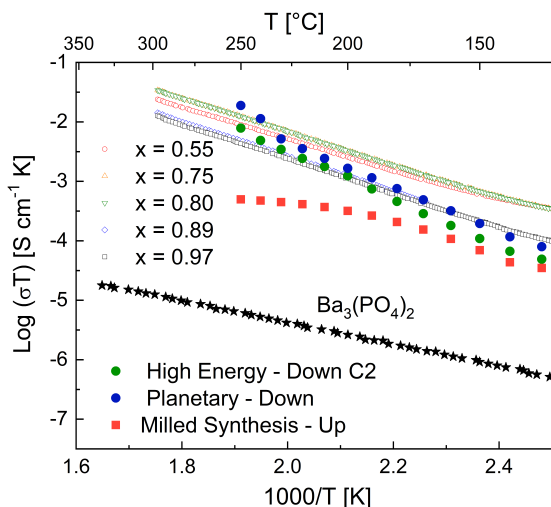


Figure 51: Milled Synthesis Arrhenius Plot

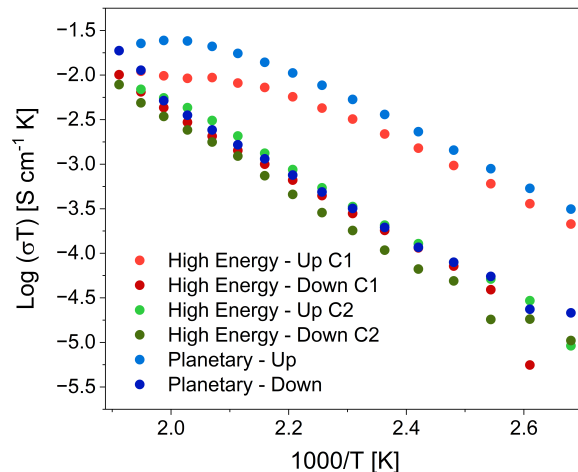


Figure 52: Arrhenius Plot

Still, taking the offset between the initial ramp up v. ramp down cycle, the milled synthesis's conductivity would still be one or two orders of magnitudes higher than that of $\text{Ba}_3(\text{PO}_4)_2$. Another measurement with the ramp down cycle measurement included will likely definitively settle the conductivity.

3.4. Future Work

It is almost certain that BKHP was not successfully synthesized via the ball mill but there are two final experiments to be done to confirm this well-founded conclusion. Producing another pellet using the technique to determine the ramp down conductivity will be helpful. Finally, milling the two potassium precursor phases can help determine why potassium ions are not shown in the diffraction pattern but exist in the washed solution.

4. Acknowledgements

The work I have done could not be completed without the insightful guidance and mentorship of Gordon Peiker. I am also incredibly grateful for Prof. Sossina Haile for allowing me to work in the lab throughout the summer. I'd also like to thank Xinqi Chen and Sumit Kewalramani for their crucial advice as instrument scientists. Finally I want to express my appreciation for the Haile Group as a whole for being incredibly welcoming.

The work I completed was supported through a National Science Foundation REU Grant.

5. Referenced Data

5.1. Single Crystal Confocal Microscope Images

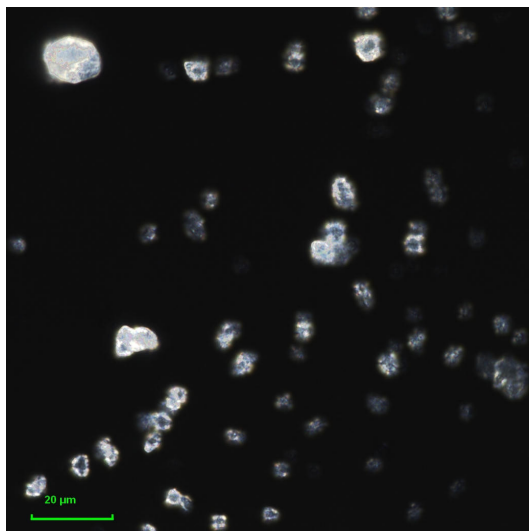


Figure 53: Planetary Milled

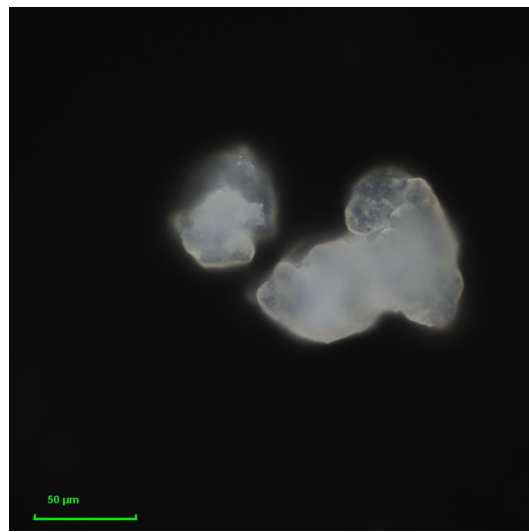


Figure 56: Pre-Mill Synthesis 2

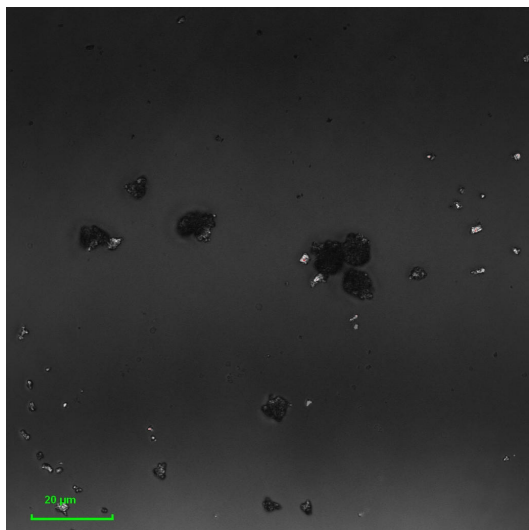


Figure 54: Bottle $\text{Ba}_3(\text{PO}_4)_2$

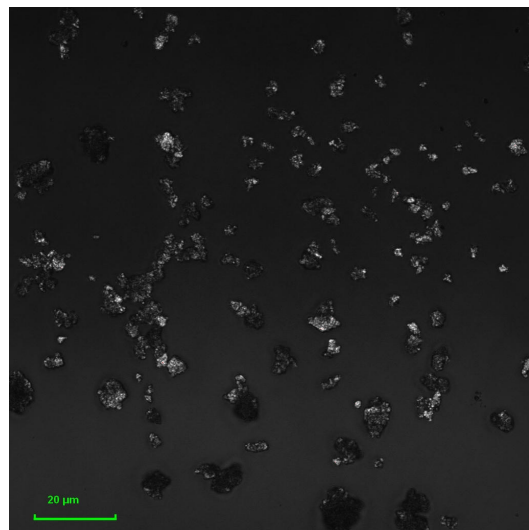


Figure 57: Bottle $\text{Ba}_3(\text{PO}_4)_2$

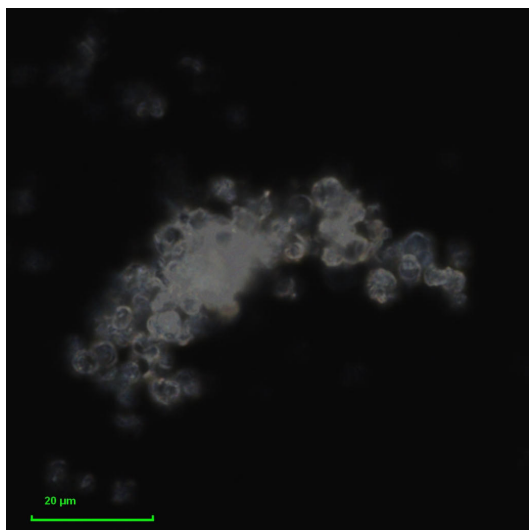


Figure 55: Pre-Mill Synthesis 1

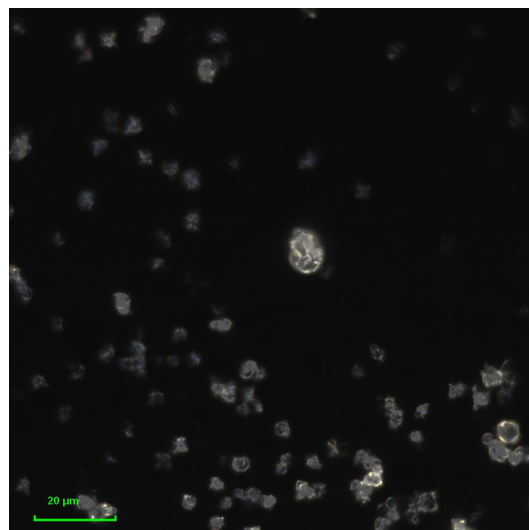


Figure 58: Pre-Mill Synthesis 2

5.1.1. Planetary Milled Pellet Intermediate Temperature Measurements

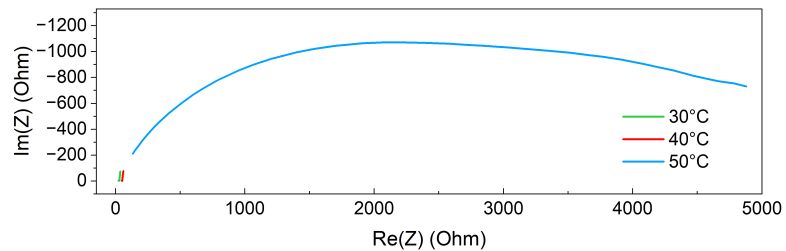


Figure 59: 30°C to 50°C Planetary Milled

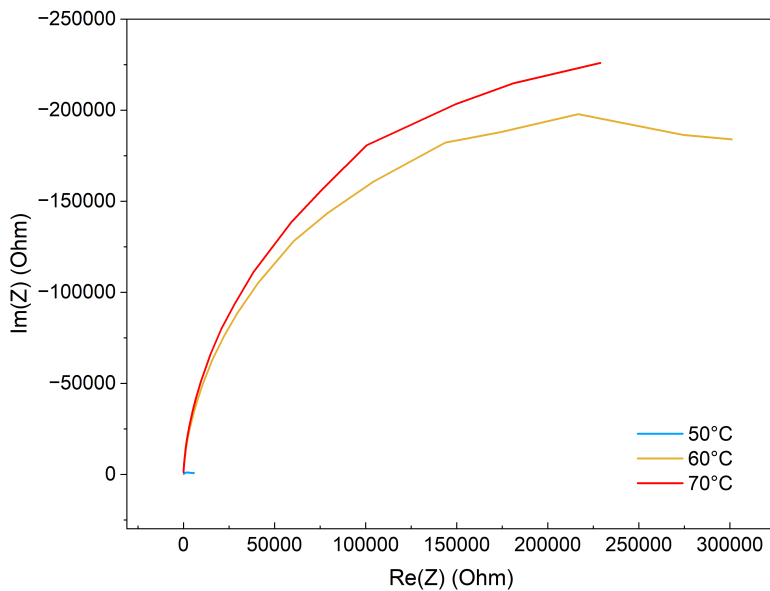


Figure 60: 50°C to 70°C Planetary Milled

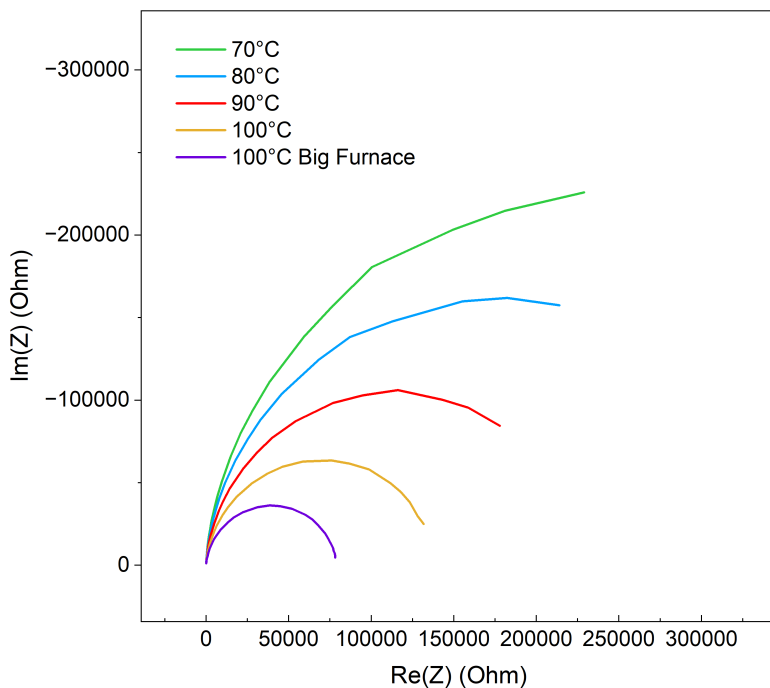


Figure 61: 70°C to 100°C Planetary Milled

5.1.2. First $x = 1$ Synthesis

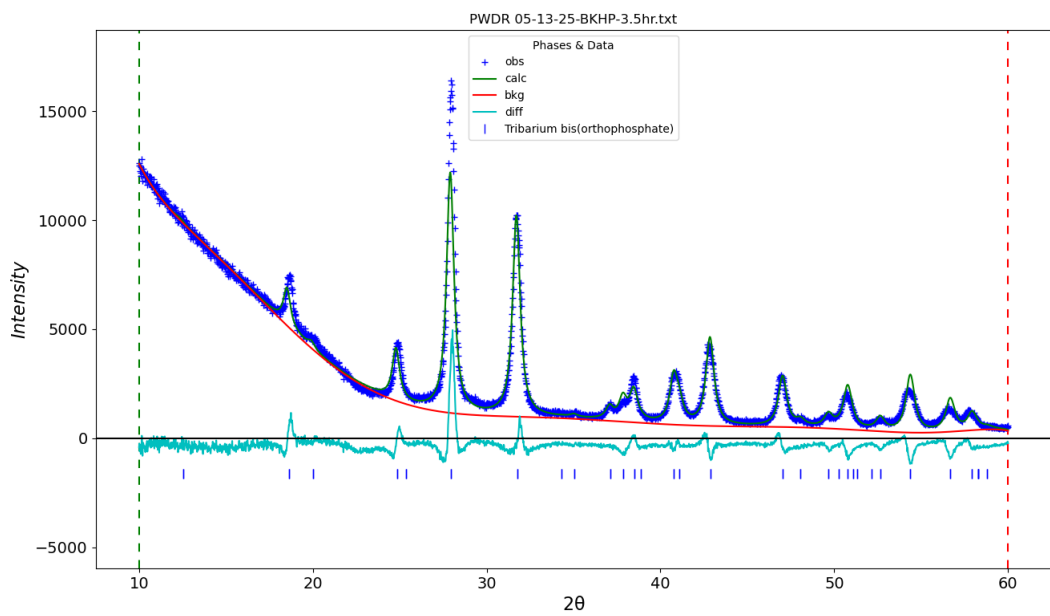


Figure 62: PXRD for Original $x = 1$ Synthesis

SAMPLE	$a(\text{\AA})$	$c(\text{\AA})$
$x = 1$	5.61508	20.98841

Table 21: Lattice Parameters from Original $x = 1$ Synthesis

6. Miscellaneous Documents

6.1. Ba₂KH(PO₄)₂ Synthesis Instructions

The following synthesis is derived from the paper attributed below.¹

6.1.1. At a glance

Precursors: barium acetate (Ba₂C₂H₃O₂), potassium hydroxide (KOH), and dipotassium hydrogen phosphate (K₂HPO₄)

- Ba₂C₂H₃O₂ solution (0.3M, 12.5mL, or 0.9578g)
- KOH solution (0.4M, 36mL, 0.8079g)
- K₂HPO₄ solution (14.6M, 36mL, 91.5469g)

KOH solution and K₂HPO₄ should be mixed to produce a potassium bearing solution with a total volume of 36mL. The combined barium and potassium solution should be stirred for 10 mins at 100°C. ≈ 0.85g of BKHP is produced from this synthesis procedure.

6.1.2. Step-by-Step Instructions

1. Measure out 0.9194g of Ba₂C₂H₃O₂ in a weigh boat
2. Measure the mass of a small beaker
3. Put the Ba₂C₂H₃O₂ into the beaker. Rinse with water and measure the total weight to calculate the water used
4. Add a total of 12mL of water into the Ba₂C₂H₃O₂ solution
5. Measure out 0.8079 g of KOH in a weigh boat
6. Measure the mass of a larger beaker
7. Put the KOH into the larger beaker
8. Measure out 91.5469g of K₂HPO₄ in a large weigh boat
9. Put the K₂HPO₄ in the larger beaker. Rinse with water to measure the total weight to calculate the water used
10. Add a total of 36mL of water to create the potassium bearing solution
11. Stir both solutions separately with a stir bar
12. After full dissolution of the two separate solutions combine and stir for 10 minutes at 90 degrees celsius
13. Set up the vacuum filtration
14. Pour the solution. Collect the filtrate to recover the potassium bearing solution
15. Wash with water multiple times and then with acetone
16. Collect a graduated cylinder and a small beaker
17. Heat the filtrate to 60-70°C and cover with a watch glass. Check occasionally the volume to ensure it reaches 36mL
18. Collect the potassium bearing solution in a Nalgene jar

6.1.3. Synthesizing with Stored Potassium Bearing Solution

Since the typical x=1 synthesis requires over 90g of K₂HPO₄, it is easy and more sustainable to reuse the potassium bearing solution. The same steps are associated with a synthesis using the stored potassium bearing solution.

¹C. R. I. Chisholm, E. S. Toberer, M. W. Louie and S. M. Haile, Chem. Mater., 2010, 22, 1186–1194.

6.2. Confocal Microscopy Sample Preparation Instructions

The following instructions is derived from the thesis attributed below.²

6.2.1. Step-by-Step Instructions

1. Measure out 5mg (0.005g) of powder sample onto a weighing paper and deposit into a small glass vial
2. Measure out $0.75\mu\text{L}$ (0.075mL) of methanol using a micropipette and deposit into each glass vial
3. Sonicate for 15 minutes.
4. Deposit $20\mu\text{L}$ of the sonicated solution onto a glass slide
5. Let air dry under the fume hood for 1 hour

²Louie, M. W. C., Electrocatalysis in Solid Acid Fuel Cells, PhD thesis, California Institute of Technology, Pasadena, CA, May 20, 2011.

Index of Figures

Figure 1 BKHP Proton Hopping	4
Figure 2 SEM BKHP Image	4
Figure 3 Pre-Milling	5
Figure 4 Post Planetary Milling	6
Figure 5 Post Planetary & High Energy Milling	6
Figure 6 Pre-Mill Synthesis 1	7
Figure 7 Pre-Mill Synthesis 2	7
Figure 8 Post Planetary Mill	7
Figure 9 Post Planetary Mill	7
Figure 10 Post Planetary Mill	7
Figure 11 Post Planetary Mill	7
Figure 12 Post Planetary & High Energy Milling	8
Figure 13 Post Planetary & High Energy Milling	8
Figure 14 Post Planetary & High Energy Milling	8
Figure 15 Post Planetary & High Energy Milling	8
Figure 16 Arrhenius Plot	10
Figure 17 Arrhenius Plot rel. Paper	10
Figure 18 Single Arc at 220°C	11
Figure 19 Planetary Milled Ramp Up Plot at 220°C & Ramp Down at 170°C	11
Figure 20 Planetary Milled Ramp Down Plot at 220°C	11
Figure 21 High Energy Milled Cycle 2 Plot at 170°C	11
Figure 22 Planetary Milled Capacitance	12
Figure 23 Pre-Ramp High Energy Milled	12
Figure 24 Pre-Ramp Planetary Milled	12
Figure 25 Post-Ramp Planetary Milled 1	12
Figure 26 Post-Ramp Planetary Milled 2	12
Figure 27 TGA & DSC Data using High Energy Milled Powder	13
Figure 28 Ambient Equilibration Measurement on Unmilled BKHP	14
Figure 29 250°C CDP v. Hydrated BKHP	14
Figure 30 30°C to 50°C Unmilled	15
Figure 31 50°C to 70°C Unmilled	15
Figure 32 70 to 100°C Unmilled	15
Figure 33 Unmilled 50°C Evolution	15
Figure 34 Planetary Milled 50°C Evolution	16
Figure 35 50°C Evolution Close-Up	16
Figure 36 Humid Arrhenius Plot	17
Figure 37 200°C BKHP at 68.94 kPa	18
Figure 38 200°C BKHP at 68.94 kPa	19
Figure 39 PXRD for Bottled Ba ₃ (PO ₄) ₂	21
Figure 40 PXRD for Bottled Ba ₃ (PO ₄) ₂ Post-Milling	21
Figure 41 PXRD for Bottled Ba ₃ (PO ₄) ₂ Post 5 Hours & 10 Minutes Milling	22
Figure 42 PXRD Data for $x = 1$ Synthesis Pre-Mill	22
Figure 43 PXRD Data for $x = 1$ Synthesis Pre-Wash & Post-Mill	23

Figure 44 PXRD Data for $x = 1$ Synthesis Post-Wash	23
Figure 45 PXRD Data for $x = 2$ Synthesis Pre-Mill	24
Figure 46 PXRD Data for $x = 2$ Synthesis Post-Mill/Pre-Wash	24
Figure 47 PXRD Data for $x = 2$ Synthesis Post-Wash	25
Figure 48 PXRD Data for Failed Potassium Occupancy Refinement with Silicon	25
Figure 49 Proton NMR Plot of Aqueous v. Ball Mill Synthesis BKHP	26
Figure 50 Proton NMR Plot from Chrisholm et. all	26
Figure 51 Milled Synthesis Arrhenius Plot	28
Figure 52 Arrhenius Plot	28
Figure 53 Planetary Milled	30
Figure 54 Bottle $\text{Ba}_3(\text{PO}_4)_2$	30
Figure 55 Pre-Mill Synthesis 1	30
Figure 56 Pre-Mill Synthesis 2	30
Figure 57 Bottle $\text{Ba}_3(\text{PO}_4)_2$	30
Figure 58 Pre-Mill Synthesis 2	30
Figure 59 30°C to 50°C Planetary Milled	31
Figure 60 50°C to 70°C Planetary Milled	31
Figure 61 70°C to 100°C Planetary Milled	31
Figure 62 PXRD for Original $x = 1$ Synthesis	32

Index of Tables

Table 1 Diffraction Lattice & Size Parameters	5
Table 2 Barium Phosphate & $x = 1$ BKHP Densities	10
Table 3 Pellet Densities	10
Table 4 Heating Profile 100 → 250°C	10
Table 5 Capacitance Values from 100 → 250°C Measurements	12
Table 6 Unmilled & Planetary Milled V2 Pellet Densities	13
Table 7 BKHP v. CDP Conductivity	14
Table 8 Heating Profile 100 → 250°C	14
Table 9 First & Second Arc Conductivity	16
Table 10 First & Second Arc Fit Results	16
Table 11 Dielectric Constant Equation	17
Table 12 150°C Humidity Measurements	18
Table 13 Precursor Mass for 2.5g of $x = 1$ BKHP	20
Table 14 $x = 1$ synthesis measurements	23
Table 15 $x = 2$ Synthesis Measurements	24
Table 16 Lattice Parameters from Chrisholm et. all	26
Table 17 Lattice Parameters from Post-Wash Milled Synthesis	26
Table 18 K ⁺ Ion Test Results	27
Table 19 Milled Synthesis Pellet Density	27
Table 20 Milled Synthesis Heating Profile 100 → 250°C	27
Table 21 Lattice Parameters from Original $x = 1$ Synthesis	32